

LIBRARY
OF THE
UNIVERSITY
OF ILLINOIS

510.84

I46r

no.156-163

cop.2

[REDACTED]



Digitized by the Internet Archive
in 2013

<http://archive.org/details/highelectricfiel159vanb>

510.87
I l6r
no. 159
cop. 2

DIGITAL COMPUTER LABORATORY
UNIVERSITY OF ILLINOIS
URBANA, ILLINOIS

REPORT NO. 159

HIGH ELECTRIC FIELD EFFECTS IN P-N JUNCTIONS
--FAST BREAKDOWNS--

by

L. van Biljon

January 20, 1964

This work was supported in part by the
Office of Naval Research under Contract No. Nonr-1834(15)

TABLE OF CONTENTS

	Page
List of Symbols	iii
Summary	v
1. INTRODUCTION	1
2. FASTEST POSSIBLE SWITCHING	4
2.1 Introduction	4
2.2 Outline of Approach	4
2.3 Junction Charge Transfer	5
2.3.1 Accelerating Force	6
2.3.2 Mobility	6
2.3.2.1 Influence of High Field	7
2.3.2.2 Average Carrier Velocity	8
2.3.2.3 Energy Transfer from Lattice	8
2.3.2.4 Mobility Due to Lattice Scattering	11
2.3.2.5 Mobility Due to Impurity Coulomb Fields	13
2.4 Transit Time	14
2.4.1 Voltage Influence on Transit Time	15
3. TRANSFER OF CHARGE PACKET ACROSS DEPLETION REGION	19
3.1 Electron Current in Depletion Region	20
4. THERMAL INFLUENCE	23
5. MICROPLASMA MODEL	25
5.1 Observed Behavior	25
5.1.1 Current-Voltage Relation	25
5.2 Electrical Equivalent Circuit	29
5.3 Energy Considerations	36
5.3.1 Determination of $\partial E/\partial t$	38
5.4 Energy Gained	42
5.5 Energy Lost to Lattice	44
5.5.1 Variation of T_1 with Time	44
5.6 Complete Expression for $\partial \epsilon/\partial t$	46
6. MICROPLASMA CHARACTERISTICS	50
6.1 General Behavior	50
6.2 Experimental Set-Up	50
6.3 First Experimental Results	52
6.4 Attempts at Using Sampling Techniques	56
6.5 Delay in Switch-On after Simulation	58
7. CONCLUSION	60
APPENDIX	62
REFERENCES	64

LIST OF SYMBOLS

A, B, C, K	constants
C	capacitance
D	diffusion constant
E	electric field strength
E_0	initial field in depletion region
E_c	critical field required for breakdown
E	kinetic energy of carrier
F	force
I	electric current
I_0	final current of a breakdown region
J	current density
L	diffusion length
M	multiplication factor
N	carrier density
N_D	donor concentration
N_A	acceptor concentration
P	rate of power dissipation
Q	electric charge
R	resistance
T	temperature
T_0	initial temperature
T_1	lattice temperature
T_2	carrier effective temperature
V	voltage
W	depletion layer width
e	base of Napierian log
k	Boltzmann constant
k'	heat conductivity of silicon
ℓ	diameter of microplasma discharge
m	mass of carrier
n	carrier concentration; integer
q	electronic charge

LIST OF SYMBOLS (CONTINUED)

$t, \Delta t$	time
u	phonon velocity in silicon at T_1
v	carrier velocity on transport
x	linear dimension
α_i	ionization coefficient
ϵ	energy
ϵ_i	ionization energy
μ	mobility
μ_i	impurity scattering mobility
μ_0	low field mobility
τ	carrier transit time; time constant

SUMMARY

The transit time of electrons across a p-n junction in which an electric field of 10^7 v/m is present is investigated and proven to be about 1 picosecond. It is shown that carrier distribution adds about 25 per cent to this time when a pulse is considered and that increasing the applied voltage does not necessarily decrease the transit time.

The energy exchange between electric field, carriers, and lattice is investigated and a cause of random pulse formation suggested from the results.

Experimental results are presented, obtained on Si junctions in which breakdowns occur. It is suggested that small breakdowns are established at speeds too fast for conventional oscilloscopes of sufficient sensitivity. It is proposed that the experimental technique of photon stimulation used here be further refined to allow the display of the true waveshape in time of micro-plasma breakdown.

1. INTRODUCTION

The application of p-n junction devices in fast switching and amplifying circuits has met with great success in many areas of electronics. However, the extreme speed of operation required of modern equipment has for some time already markedly influenced the design and fabrication of special semiconductor units in an endeavor to increase their speed. By these requirements, transistors and diodes have been taken into the nanosecond region and at the present time, this order of magnitude seems the limit attainable with existing devices.

A pulse rise time of one or more nanoseconds is considered fast, and a fall time of this duration is relatively difficult to obtain with transistors.

Compromising depletion layer capacitance and spreading resistance for a junction still capable of practical currents without excessive temperature rise, produces junction constants severely limiting the speed of response. A capacitance of 2 to 5 pf with an effective series resistance of between 20 and 200 ohms is becoming common so that the basic RC rise time is of the order of a nanosecond or two. Some time ago¹ avalanche circuits of special design proved capable of fractional nanosecond rise time but the fall time was about an order or more longer. With ever better junctions becoming available, avalanche breakdown seems to hold much promise of doing considerably better than has been achieved up to now. The special response characteristics of "hard" breakdown junctions hold promise of successful application in picosecond circuits, possibly proving a breakthrough as far as junction speed is concerned.

The salient features of this special "plasma" type of breakdown (being termed either micro- or macroplasma rather arbitrarily, depending upon the cross-section of the breakdown) are the following:

Extreme speed of current build-up^{2,3,4} (10^{-12} sec).

Practically no junction voltage change, thus limiting charging time for depletion layer capacitances.

Extreme speed of current switch-off⁵ (10^{-11} sec).

Apart from the desirable characteristics mentioned above the following attributes of this type of breakdown greatly enhance its usefulness in all types of electronic circuitry:

Square, amplitude limited pulses are produced (see Fig. 1).

The average "on" or "off" ratio in the pulse train is smoothly variable from zero to infinite (see Fig. 10).

The pulse formation and extinction is accompanied by photon emission.

Pulse formation is directly influenced by the presence of photons or other ionizing agents.

This report deals with some aspects of this type of junction breakdown as observed in silicon structures. The diodes used in this investigation were kindly donated by the Shockley Transistor Laboratories of the Clevite Company, Palo Alto, California.



Current pulse with voltage just above breakdown value.

Horizontal: 10 microsec/cm
Vertical: 20 microamp/cm



Current pulse with voltage about 50 mv above breakdown value.

Horizontal: 10 microsec/cm
Vertical: 20 microamp/cm

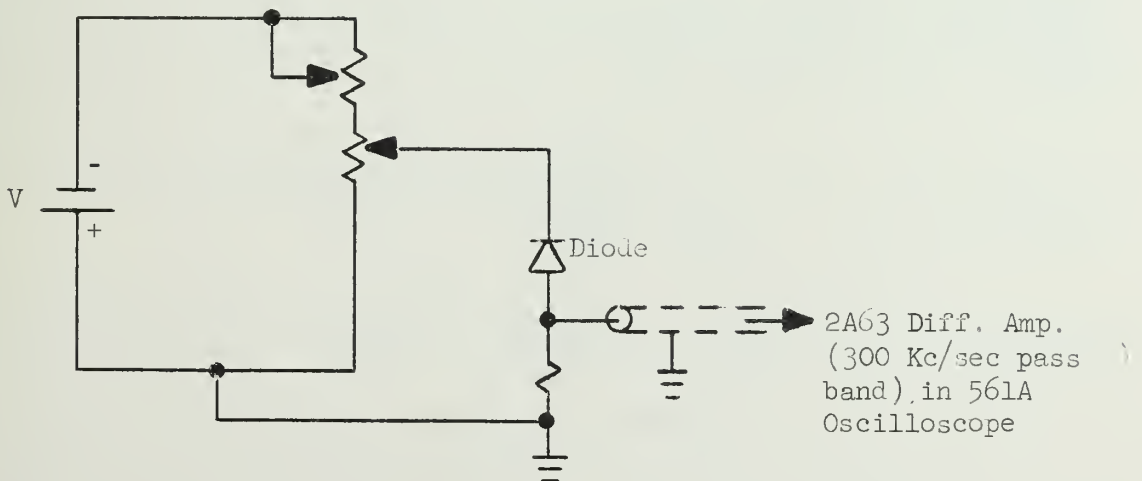


Figure 1. Typical Breakdown Current Pulses in Si Junction

2. FASTEST POSSIBLE SWITCHING

2.1 Introduction

It is proposed to analyze the fastest possible response obtainable with a p-n junction. This entails firstly a study of the speed of transfer of charge carriers across a junction as well as the shape of a charge packet traversing the depletion region.

The phenomena of microplasma formation is coupled to a first-order analysis of thermal effects in the junction while in a separate section due consideration is given to RC time constant effects.

2.2 Outline of Approach

Conventional p-n junctions used in high-frequency applications have a depletion layer capacitance of the order of 5 pf. Many factors militate against the reduction of this figure without sacrifice of speed. Lowering the capacitance by having a wider depletion width requires higher resistivity material to be used, thus increasing series spreading resistance. Also, decreasing the junction area poses severe technological difficulties as well as imposing current limitations due to thermal effects.

A present-day compromise indicates a junction depletion layer capacitance of about 5 pf and a spreading resistance of about 50 ohms. An RC time of about one-half nanosecond thus results meaning that it will be difficult to adequately pass pulses of around one or two nanosecond duration.

It seems at present that the only way of utilizing existing junctions at speeds faster than those mentioned above is to have them operate in the so-called "microplasma" breakdown region.

The phenomenon of microplasma formation has been observed by many workers and several models for this type of operation have been proposed.^{6,7,8}

The definite advantages of this mode of operation are the following:

The effective, active area of the junction is greatly reduced; typical microplasmas have diameters of 2 or 3 micron.

While going from "on" to "off" and vice versa, the voltage across the discharge region hardly changes; this eliminates

much of the need for transport of charges to and from the effective junction depletion layer capacitance.

An avalanche type of breakdown characteristic provides extremely fast current build-up; estimated rise times are of the order of 10^{-12} seconds (see paragraph 2.4).

At present the most severe disadvantage of this operating mode is that junctions exhibiting this phenomenon reliably are not readily available. Recent developments⁹ though indicate that this is a temporary situation. The long-standing objection to avalanche operation, that of thermal run-away, is also fast being eliminated by the production of near-perfect low saturation current junctions. Silicon junctions have been operated in the microplasma mode for several hours without noticeable tendency towards runaway or change in characteristics.

In this report an evaluation is made of the more important factors influencing microplasma behavior of p-n junctions.

2.3 Junction Charge Transfer

The charge transfer to be considered here differs from conventional charged particles acted upon by an electric field in that due consideration has to be given to the fact that such intense electric fields are present that the mobility is affected.

Consider the simplest possible model--a depletion region of width W , in series with a pure voltage source V , and no extra resistance in the circuit.

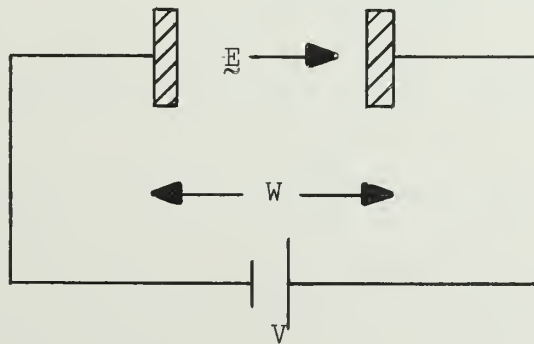


Figure 2. Simple Model Considered

Consider as a starting point the transfer of a single charged particle across the depletion region.

The velocity of transport will depend upon three main factors, viz.:

Accelerating force

Mean free path

Mobility

These factors have to be briefly considered more closely.

2.3.1 Accelerating Force

$$\text{Force} = \text{Charge} \times \text{Field Strength}$$

If each discrete charge is equal to q , the force will be F , where:

$$F = q \cdot E \quad (1)$$

and

$$E = (V/W) \text{ volts/meter}$$

2.3.2 Mobility

In its simplest form the mobility is expressed as the velocity resulting from unit field strength, i.e.,

$$\mu = v/E \quad (\text{meters/sec}) \text{ per } (\text{volt/meter})$$

In a first-order approach one could find the mobility by stating:

$$q \cdot E \simeq m \cdot \ddot{x}$$

and by assuming a mean free time τ , the distance travelled in this time may be found by twice integrating the above to give:

$$x = \frac{q\tilde{E}}{2m} \tau^2$$

and since

$$\tilde{v} = \frac{x}{\tau}$$

the mobility follows as:

$$\mu = \frac{x}{\tau \tilde{E}} = \frac{q\tau}{2m} \quad (2)$$

Now, equation (2), denoting an average mobility is perfectly in order while the field strength in the depletion region is relatively low--of the order of 10^6 volts/meter.

At higher fields, however, the energy gained by the carriers from the field during a mean free time, may be a significant fraction of the mean carrier energy (i.e., $3/2 kT$) so that the lattice and the carriers are not in thermal equilibrium any more. It thus becomes necessary to consider the mobility as a function of the field strength in the depletion region.

2.3.2.1 Influence of High Field

The field strength influences the mobility mainly through influence of the mean velocity.

As before, the mobility may be defined by

$$\mu = \frac{\tilde{v}}{\tilde{E}}$$

but the average velocity \tilde{v} needs to be considered further.

2.3.2.2 Average Carrier Velocity

Carriers obtain their energy mainly in two ways:

Direct interaction with the electric field.

Scattering by the lattice and by impurity centers.

Interaction with the electric field was mentioned in paragraph 2.3.1 so that now the two scattering mechanisms have to be evaluated.

At room temperature, impurity scattering is highly elastic and thus not important for energy transfer considerations. However, in present-day structures, it has been observed (see paragraph 6.3) that better microplasma response is obtained at low ambient temperatures (e.g., that of liquid nitrogen) so that in a more complete analysis elastic scattering may not be assumed.

2.3.2.3 Energy Transfer from Lattice

Let attention be confined to electrons as the mobile carriers in the depletion region.

It may be shown that in a crystal at temperature T_1 (i.e., lattice temperature T_1), the average energy gain $d\epsilon$, upon scattering is given by:¹⁰

$$d\epsilon = 4mu^2 \left[1 - \frac{E'}{2kT_1} \right] \quad (3)$$

where

m = mass of electron

u = velocity of sound in crystal

k = Boltzmann's constant

E' = K.E. of particle prior to collision with lattice

However, where (3) gives the average energy gain, it now becomes necessary also to use the concept of "effective" temperature and velocity.

A reasonable assumption at the outset is that the particles in the depletion region have a Maxwellian velocity distribution.^{10,11} For a total number of carriers N , the number having velocities between v and $(v + dv)$ will be given by:

$$\frac{4N}{\alpha^3 \sqrt{\pi}} v^2 e^{-\frac{v^2}{\alpha^2}} \cdot dv$$

where α is some constant.

Assigning to α the value indicated by Smith (loc. cit. page 159) the complete expression for the number of carriers in the velocity interval dv , will be:

$$N(v)dv = \frac{m}{(2\pi RT_2)^{3/2}} e^{-\frac{mv^2}{2kT_2}} \cdot v^2 dv \quad (4)$$

where

R = gas constant

T_2 = effective temperature of particles, and at high temperatures $T_2 > T_1$

If now a particle, in this case an electron, travels a mean free path λ , in the depletion region at a velocity v , the collision rate will be

$$\text{Collisions/unit time} = \frac{v}{\lambda}$$

and the mean rate of energy gain per particle will be

$$\left(\frac{v}{\lambda} \right) d\epsilon$$

This may be averaged for all particles so that the average rate of energy exchange will be:

$$\begin{aligned}
 \left. \frac{d\epsilon}{dt} \right|_{\text{all particles}} &= \left[\frac{\text{Total gain}}{\text{Total number of particles}} \right] = - \frac{\int_0^\alpha N(\tilde{v}) d\tilde{v} \cdot d\epsilon}{\int_0^\alpha N(\tilde{v}) d\tilde{v}} \\
 &= \frac{\frac{1}{\lambda} \int_0^\alpha \frac{4m^2 u^2}{(2\pi RT_2)^{1/2}} \left[1 - \frac{E}{2kT_1} \right] \cdot e^{-\frac{m\tilde{v}^2}{2kT_2}} \cdot \tilde{v}^3 d\tilde{v}}{\int_0^\alpha \frac{m}{(2\pi RT_2)^{1/2}} \cdot e^{-\frac{m\tilde{v}^2}{2kT_2}} \cdot \tilde{v}^2 d\tilde{v}} \quad (5) \\
 &= A \cdot \frac{\int_0^\alpha (\tilde{v}^3 \cdot e^{-B\tilde{v}^2} - C\tilde{v}^5 e^{-B\tilde{v}^2}) d\tilde{v}}{\int_0^\alpha \tilde{v}^2 e^{-B\tilde{v}^2} d\tilde{v}}
 \end{aligned}$$

where

$$A = \frac{4mu^2}{\lambda}$$

$$B = \frac{m}{2kT_2}$$

$$C = \frac{m}{4kT_1}$$

$$E = \frac{1}{2} m\tilde{v}^2$$

As shown in the Appendix (page 62) the integrals may be evaluated to give

$$\frac{d\epsilon}{dt} = A \cdot \left[\frac{\frac{1}{2B^2} - \frac{C}{B^3}}{\frac{1}{4B} \sqrt{\pi/B}} \right]$$

i.e.,

$$\frac{d\epsilon}{dt} = \frac{16kT_2 u^2}{\lambda} \sqrt{\frac{m}{2kT_2 \pi}} \left(1 - \frac{T_2}{T_1} \right) \quad (6)$$

Equation (6) shows that if

$$T_2 = T_1$$

no net transfer of energy will take place between electrons and the lattice, i.e., thermal equilibrium prevails.

2.3.2.4 Mobility Due to Lattice Scattering

Knowing the rate of energy transfer between thermal lattice energy and the carriers in the depletion region, the influence of the electric field on the mobility may now be found. This seems best done with the help of the concept of effective temperature, where this temperature is a measure of the mobility.

In the general case of electrons crossing a depletion region under the action of an electric field \mathcal{E} , the rate of energy gain may be written as:

$$\left. \frac{d\epsilon}{dt} \right|_{\text{gained from } \mathcal{E}} = \text{Force} \times \text{Average velocity} \simeq q\mu\mathcal{E}^2 \quad (7)$$

In (7), μ is the effective mobility and the relation above is only approximately true, since in a high field region diffusion may also play a part in carrier transport. For the present, however, only field effects will be considered; especially if the current is relatively small, will this be a reasonable assumption. A characteristic of microplasma currents on the other hand is that

of extreme current density, and this may require a diffusion correction to the drift expression. In the interest of simplicity, this will not be considered in the present analysis.

Contemplation of the physical model assumed for current flow in the depletion region and the interaction between the carriers and the crystal lattice makes it apparent that the direction of energy transfer, obviously determined by the relative effective temperatures, is not immediately obvious.

The very simplest case will be that where the energy gained by the carriers from the field is all dissipated in collisions with the lattice, i.e.,

$$\left. \frac{\partial \epsilon}{\partial t} \right|_{\text{from } \mathbb{E}} + \left. \frac{\partial \epsilon}{\partial t} \right|_{\text{from lattice}} = 0 \quad (8)$$

Equation (8) indicates an equilibrium condition--a steady temperature will have been reached and no net transfer of energy takes place. This obviously is a first-order assumption, and does not take account of the impurities. However, a solution which does not make use of this kind of simplification becomes prohibitively complicated with a seemingly small gain in accuracy.

Smith¹⁰ has shown that by using this simplification the effective lattice mobility may be expressed as a function of the low field mobility μ_0 and as a function of the ratio of the lattice to effective electron temperature, in the form:

$$\mu = \mu_0 \sqrt{\frac{T_1}{T_2}} \quad (9)$$

The relation between the two temperatures has been given as a function of the electric field \mathbb{E} , by Shockley¹² as:

$$\left(\frac{T_2}{T_1} \right)^2 - \frac{T_2}{T_1} - \frac{3\pi}{32} \left(\frac{\mu \cdot \mathbb{E}}{u} \right)^2 = 0$$

which may be solved for $\left(\frac{T_2}{T_1} \right)$ in the usual way to give:

$$\frac{T_2}{T_1} = \frac{1}{2} \left[1 + \sqrt{\frac{3\pi}{8} \left(\frac{\mu_0 E}{u} \right)^2} \right] \quad (10)$$

In the presence of very high fields, like those encountered in junctions where microplasmas form, the following inequality holds:

$$E \gg \left(\frac{\mu_0}{u} \right)$$

From (9) and (10) the mobility due to lattice scattering in the depletion region is thus found to be

$$\mu_l \approx \sqrt{\frac{32}{3\pi}} \sqrt{\frac{\mu_0 u}{E}} \quad (11)$$

2.3.2.5 Mobility Due to Impurity Coulomb Fields

Either the classical analysis of Mott and Massey¹³ or the more recent work of Conwell¹⁴ (and Weiskopff) or that of Dingle¹⁵ and Brooks¹⁶ may be applied, but their results are not widely different.

The first two analyses mentioned lead to what is now commonly known as the Conwell-Weiskopff formula; the remaining analyses have in common with the former that they lead to equally unwieldy expressions.

However, using values given by Conwell:¹⁴

$$\mu_i = 8.5 \times 10^{17} \sqrt{\frac{m}{m_e}} \frac{T^{3/2}}{N_i \ln \left[1 + 8.3 \times 10^8 \frac{T^2}{N_i^{3/2}} \right]} \quad (12)$$

The mass ratio $\left(\frac{m_e}{m} \right)$ has been determined by cyclotron resonance methods by several workers, and for electrons in S_i , this value may be taken to be about 0.4.

Also

$$N_i = 10^{15}/\text{cm}^3$$

$$T = 78^\circ\text{K (liquid nitrogen)}$$

and for equation (11), the parameters may be assigned values¹⁰

$$\mu_0 = 0.135 \text{ m}^2/\text{volt sec}$$

$$u = 5 \times 10^3 \text{ m/sec}$$

$$E = 10^7 \text{ v/m}$$

The two mobilities thus are computed to be:

$$\mu_\ell = 0.01 \text{ m}^2/\text{volt sec}$$

$$\mu_i = 0.41 \text{ m}^2/\text{volt sec}$$

and they may be combined by the approximate relation:¹¹

$$\frac{1}{\mu} = \frac{1}{\mu_\ell} + \frac{1}{\mu_i} \quad (13)$$

whence:

$$\mu = 0.098 \text{ m}^2/\text{volt sec} \quad (14)$$

It is important to note from the above that according to this approach, the impurity scattering greatly reduces the effective mobility and furthermore that the lattice mobility decreases rather sharply at high values of depletion layer field strength.

2.4 Transit Time

Knowing the carrier mobility and the dimensions of the depletion region, the transit time of charges across the high field region may be computed.

The transit time, T , is given by:

$$T = \frac{W}{v}$$

where

$$\underline{v} = \mu \underline{E}$$

From the values quoted above, follows:

$$\underline{v} = 0.098 \times 10^7 \simeq 10^6 \text{ m/sec}$$

while in the units presently under test, the depletion layer width, at breakdown is about

$$W = 10^{-6} \text{ meter}$$

Therefore

$$T = \frac{10^{-6}}{10^6} = 1 \text{ picosecond}$$

Transit times of this order of magnitude have been predicted by Salzberg and Sard,² although no calculations were given.

2.4.1 Voltage Influence on Transit Time

It is interesting to note the probable variation of transit time with applied voltage and the possibility of decreasing the charge transit time by increasing the junction voltage.

It is assumed that the impurity scattering mobility may be considered independent of the field but the lattice mobility as mentioned decreases with \underline{E} .

In particular,

$$\mu_l = K_1 \frac{1}{\sqrt{\underline{E}}}$$

where K_1 is a constant, and from equation (11) this gives:

$$\mu_{\ell} = \frac{35.1}{\sqrt{E}} \text{ m}^2/\text{volt sec}$$

From equation (14):

$$\mu = \frac{\mu_{\ell}\mu_i}{\mu_{\ell} + \mu_i} \simeq \left(\frac{35 \times \mu_i}{35 + \mu_i\sqrt{E}} \right) \text{ m}^2/\text{volt sec} \quad (15)$$

In equation (15) it may be noted that the fields presently under consideration are larger than 10^6 v/m so that with a μ_i of 0.41

$$\mu_i\sqrt{E} \gg 35$$

whence from equation (13):

$$\mu \simeq \frac{35}{\sqrt{E}} \text{ m}^2/\text{volt sec}$$

The velocity of transport thus follows as:

$$v = \mu E = 35\sqrt{E}$$

At this stage it should be recalled, though, that the field E is not only a function of the applied external voltage, but also of the width of the depletion region, i.e.,

$$E = \frac{V}{W}$$

where $W = K_2\sqrt{V}$ and K_2 is a constant. Thus

$$E = \frac{1}{K_2}\sqrt{V}$$

whence

$$v = K_3 \sqrt[4]{V}$$

The transit time, T, which is expressed by W/v , will thus take the form:

$$T = \frac{K_2 \sqrt{V}}{K_3 \sqrt[4]{V}} = K_5 \sqrt[4]{V} \quad (16)$$

From equation (16) it is seen that a high voltages no gain in transit time is accomplished by increasing the applied voltage. In fact, considering the non-linear relation between mobility and field strength, it may be possible to derive an optimum applied voltage for a specific junction in order to ensure minimum transit time. The law relating W to V for the specific junction will, however, first have to be determined for every specific case.

Due to the approximate nature of this type of analysis a word of caution regarding interpretation is in order. An extension of the ideas leading up to equation (11) illustrates this point.

Smith,¹⁰ for instance, proves that by using the ideas mentioned in the preceding paragraphs, the high field mobility may be expressed in terms of the low field mobility according to the expression:

$$\mu = \mu_0 [1 - \alpha E^2]$$

where

$$\alpha = \frac{3\pi}{64\mu^2} \mu_0^2$$

Using the approximate values of

$$\mu_0 = 0.135 \text{ m}^2/\text{volt sec}$$

$$u = 5 \times 10^3 \text{ m/sec}$$

it follows that

$$\mu \rightarrow 0$$

when

$$\mathbb{E} \rightarrow 10^5 \text{ v/m}$$

As this is not supported by experimental observation it is obvious that the model is restricted in its validity.

3. TRANSFER OF CHARGE PACKET ACROSS DEPLETION REGION

The results derived above apply to the behavior of an average carrier. It remains to be determined what spread there may be in time if a charge packet crosses the depletion region. If this spread is appreciable the current build-up in time will be adversely affected at the output of the device.

In order to make analysis possible, it is necessary to simplify the model somewhat.

It is assumed that a depletion region of width W is present. The microplasma discharge is now assumed to occur in the center of this region and to have dimensions negligible compared to the depletion width.

This result is partly supported by results reported by Chynoweth¹⁷ who has found that in a depletion width of W , where the ionization coefficient is $\alpha_i(E)$, the multiplication factor M follows the law:

$$1 - \frac{1}{M} \approx 0.3\alpha_i(E) \cdot W$$

indicating that ionization takes place only in about one-third of the depletion width. Although being by no means negligible compared to the depletion width the "source" of charges does seem to be a localized effect. Furthermore, since the ionization coefficient increases with electric field strength maximum ionization is more likely to occur where the field is strongest, i.e., in the center of the depletion region.

Considering also that both holes and electrons have to be accelerated before achieving ionizing energies, it is conceivable that ionization will not take place near the depletion layer edges where carriers have just entered the high field region. This implies also that carriers entering one end of the depletion region will not require the total depletion width for acceleration to ionizing energies due to the factor "0.3" mentioned above.

In this simplified model then, an infinitely narrow charge packet now starts at $x = W/2$, is acted on by the field, and it is required to know what its dimensions are at $x = W$.

This problem is well known in the study of electron packet propagation in vacuum tubes but it should be remembered that in the present case there are two significant differences between this and the electron packet problem. First, the microplasma essentially creates two charge packets travelling in opposite directions, while the transit of the field region now also is not in a vacuum but through a medium containing atoms capable of yielding free carriers when excited.

The spread in charge distribution in space is smaller for small mobilities than for larger ones, and the biggest spread will thus occur for the electron packet. The more diffused packet will probably take the longer time to traverse the edge of the depletion region thus being the slower rising current pulse; (this however is also affected by the ratio of the mobilities of the two types of carriers.).

3.1 Electron Current in Depletion Region

In keeping with the idea of a simplified model a constant electric field will be assumed in the depletion region. The continuity equation for electrons, neglecting recombination in this high field region, will be:

$$\frac{\partial n}{\partial t} = D \cdot \nabla^2 n \quad (17)$$

Noting that "n" here signifies the deviation from the equilibrium level of electron density, this equation is seen to be identical to the general heat flow expression.

If at time $t = 0$, the flow starts, while the electron packet has negligible dimensions, the standard result from the theory of heat flow²³ indicates a solution at any subsequent instant t , as:

$$n = \frac{N}{K_1 \sqrt{t}} e^{-\frac{x^2}{K_2 t}}$$

where k_1 and k_2 are constants and N is the total number of electrons in the packet

For the case of electrons moving in a semiconductor, the constants k_1 and k_2 may be evaluated to have n read

$$n = \frac{N}{\sqrt{4\pi Dt}} e^{-\frac{x^2}{4Dt}} \quad (18)$$

However, contemplation of equation (18) shows that the influence of the electric field has been neglected, while it is intuitively felt that its influence will be to increase the x-coordinate of the (center of the) charge packet.

If x is the true coordinate at time t, while it would have been x' in the absence of the field, one may write:

$$x = x' + \mu Et$$

As for the solution for n in equation (18) however, the packet will only have diffused the effective distance x' , so that x in (18) should be replaced by:

$$x' = x - \mu Et$$

whence:

$$n = \frac{N}{\sqrt{4\pi Dt}} e^{-\frac{(x-\mu Et)^2}{4Dt}} \quad (19)$$

Consider now the shape in x, of n at any instant t. Let the pulse have moved from $x = 0$, where it started at $t = 0$, to some point where it is momentarily frozen so as to observe its shape.

Equation (19) shows that the spread of the pulse between its $(1/e)$ points from the central peak is of the order of

$$2x \sqrt{4Dt} = \Delta x$$

Consider now the order of time taken to move this distance (Fig. 3).

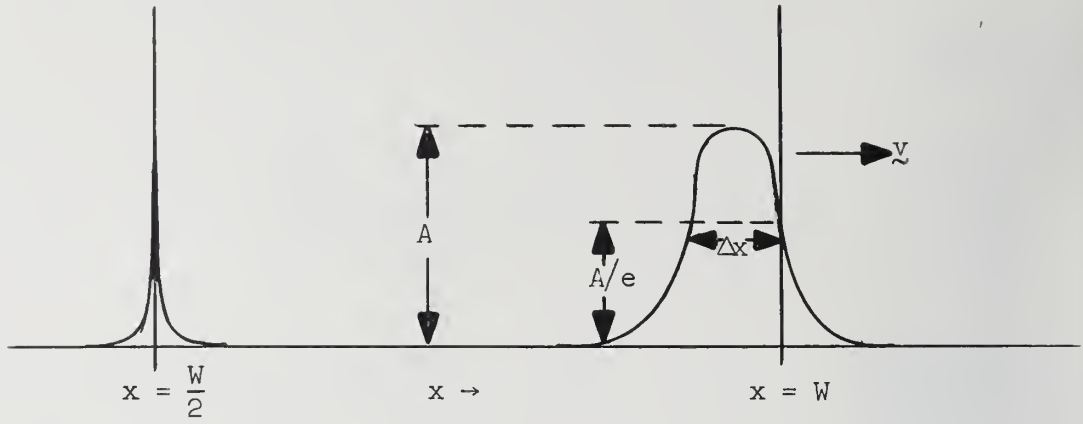


Figure 3

First assume that the pulse has moved from the center of the depletion region to its edge--the previous analysis has shown that this takes a time of about 10^{-12} seconds to happen.

Δx is thus found to be:

$$\Delta x = 4 \sqrt{35 \times 10^{-4} \times 10^{-12}} \simeq 24 \times 10^{-8} \text{ meters}$$

The mean drift velocity had been found as

$$\bar{v} = 10^6 \text{ m/sec}$$

so that the time for the pulse to move across the edge of the depletion region from one $(1/e)$ point to the other is:

$$\Delta t = \frac{\Delta x}{\bar{v}} = \frac{24 \times 10^{-8}}{10^6} < 0.24 \text{ picosecond}$$

This result indicates that although an average carrier will take about one picosecond to cross the depletion region, about 25 per cent more time will be required for the total pulse to pass due to spread in particle position.

4. THERMAL INFLUENCE

It is believed that thermal influences are of the utmost importance in junction breakdown, especially in microplasma-type breakdowns. This will be referred to again quite extensively at a later stage, but a brief indication of its probable importance will be in order now.

Microplasmas occur in present-day Si junctions at voltages typically of the order of 20 to 40 volts. The current carried by a single microplasma has been reported by several authors to be in the 10 to 200 microampere range.

Take as a representative case

$$V = 30 \text{ volts}$$

$$I = 50 \text{ microamp}$$

The rate of dissipation will be $V \times I = 1500$ microwatts.

A "typical" "ON" time for a microplasma does not exist, but take as an example the practical figure of a discharge that remains on for one microsecond.

The total dissipation will thus be

$$1500 \times 10^{-12} \text{ joules} = 1.5 \times 10^{-9} \text{ joules}$$

This is then the energy expended within the volume of a single microplasma,

The actual physical dimensions of the active discharge region are still somewhat in doubt but it is reasonable to assume from published data,¹⁸ that this region has a cylindrical shape of length equal to its diameter, equal to one micron. The microplasma volume thus is about 10^{-18} cubic meters. The specific gravity of Si is about 2.33 whence the weight of the microplasma volume is of the order of

$$2.3 \times 10^{-15} \text{ kgm}$$

The specific heat is quoted as $760 \text{ joules/kgm}^\circ\text{C}$ so that the dissipation of 1.5×10^{-9} joules, could, if negligible heat were lost to the surroundings, raise the temperature by ΔT , where:

$$\Delta T \simeq 900^{\circ}\text{C}$$

This temperatures which is of the order of 75 per cent of the melting point of Si seems very high, but could thus be approached, depending upon the thermal time constants of the regions involved. It should be remembered that the temperature rise above was the consequence of a single current pulse. Depending on the pulse repetition frequency, higher temperatures are conceivable. Rose⁶ calculates an approximate rise in temperatures of about 40°C but stresses that this may be conservative. He assumes a thermal time constant of about 10^{-11} secs. Considering, however, some considerable experimental evidence on microplasmas which has become available, some aspects of the thermal behavior of microplasmas are far from clear. For instance, the original microplasma model of Rose⁶ assumed a high field in the regions flanking the actual discharge volume; due to high ionization density in the latter volume, the voltage across it could not be very high.

Shockley's¹⁸ model looks somewhat like Rose's and he calculates a space charge resistance of the order of 10^4 ohms but with a microplasma current of 100 microamperes, this accounts for only one volt of the applied voltage. Shockley also calculated the spreading resistance of the two regions bordering on the discharge, but finds this bulk material resistance an order of magnitude less than the space charge resistance.

It seems that the only probable solution could be that either the space charge resistance seems higher than predicted with the present model, or that rather severe deviations from Ohm's law occurs in the breakdown region. Keeping in mind these possible effects, it is nevertheless felt that, in the light of experimental evidence (see paragraph 6) thermal effects play a much more important role than thus far ascribed to them.

5. MICROPLASMA MODEL

5.1 Observed Behavior

Considering the current-voltage relation of a junction showing clear microplasma behavior, the most striking features, initially, is the very "hard" characteristic (Fig. 4).

Typically a reverse diode resistance of 1000 Megohm or more is found below breakdown; at and just above breakdown the resistance is difficult to determined, since the current pulse shape is still in doubt. Oscillograms indicate, however, that this latter resistance is relatively high, of the order of tens of thousands of ohms.

5.1.1 Current-Voltage Relation

One of the most complete discussions of microplasma V-I characteristics has been given by Haitz¹⁹ based to a large extent on the model proposed by Champlin.⁸

This model has among others, the following characteristics: if the junction voltages rises above a certain critical value V_B , the microplasma may switch on. On the average, it waits a time t_0 before doing so and carries a current I . When the voltage drops below V_B , the microplasma switches off immediately. Two points may be raised here; the first is the abrupt switching off. Although both "on" and "off" switching has been found to be fast, the "off" time invariably is longer. That this effect may have a thermal origin is suggested by the experimentally observed decrease in switching off time at low ambient temperature (Fig. 11). However, if recombination plays an important role in switch-off as suggested by Jonscher,²⁴ this process could be fast.

The second point, and one of considerable practical important is the fact that Champlin,⁸ and others, have observed an average time lag t_0 after the critical voltage has been reached, before the breakdown sets in.

In any fast application this delay, which has been claimed to be of the order of a microsecond by Champlin, would render the phenomenon quite useless. It is thus essential that this delay must either be eliminated, or for present applications, reduced to at most say 1 picosecond. It is thought

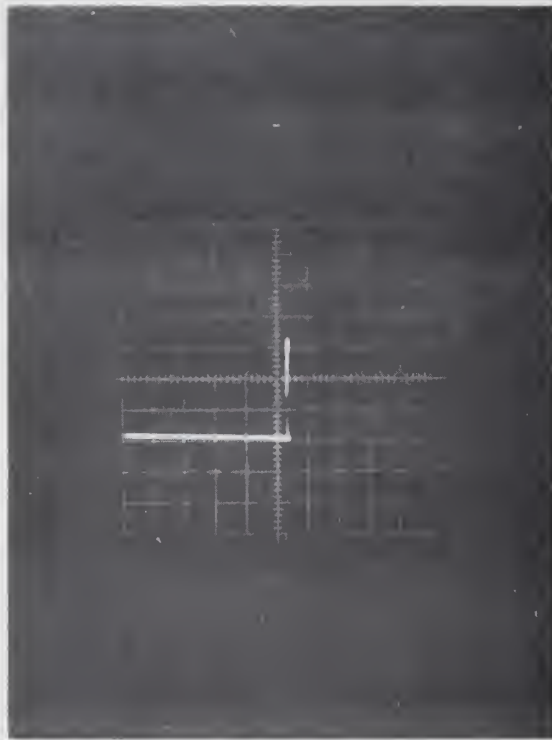


Figure 4. Si p-n Junction V-I Characteristic

Horizontal: 4 volts/cm

Vertical: 5 microamp/cm

(Tektronix Transistor Curve Tracer
at 240 c/sec)

that this delay is caused by the fact that although a sufficiently high field may be present in the depletion region, the arrival of an initiating carrier has to be awaited.

It is contended now that the discharge will appear immediately, even in the absence of an externally derived initiating carrier, if a carrier could be released within the confines of the depletion region. This could be done by sufficiently raising the applied voltage to release carriers by field emission, or by injecting photons to energize potential ionizing carriers.

The likelihood of this being the case is supported by the observed variation of the function ϕ_{10} (Champlin⁸) from 0 to infinity over some small voltage range; this means that at some value of the field the discharge cannot extinguish since initiating carriers are always present. That it might be wanting to extinguish may be illustrated by the high noise content of this current. The heat generated by the current pulse cannot be neglected. Rose⁶ calculated the thermal time constant of a microplasma region to be of the order of 10^{-11} seconds, so that no sluggishness need be introduced by the thermal action, on the present time scale.

Of particular importance is the fact that in a bistable microplasma the turn-off probability sharply decreases with breakdown area, i.e., with current. Since the ΔV 's involved seem small, a change of ΔA in area would mean a change of (constant ΔA) current but a $(\text{constant} \times \Delta A)^2$ in dissipation; it might thus be that the higher local temperature keeps the discharge going by supplying carriers. This view is further supported by the slope of the turn-off probability vs. current curves. In Fig. 5 are shown some approximate curves of results obtained by Haitz¹⁹ and by McIntyre.³

Considering the three units shown, it is obvious that at higher currents, when the ambient temperature will be higher, the turn-off probability is less dependent upon current.

Another point, however, is that higher ambient temperature, at fixed depletion layer field (or rather, fixed applied voltage), tends to extinguish the microplasmas. This is a very marked effect as the following figures will illustrate: A silicon junction breaks down completely (i.e., ϕ_{10} is zero) at 25.1 volts when the ambient temperature is 300°K. When this same junction is at 360°K the same condition is only obtained at 25.9 volts. This conforms with

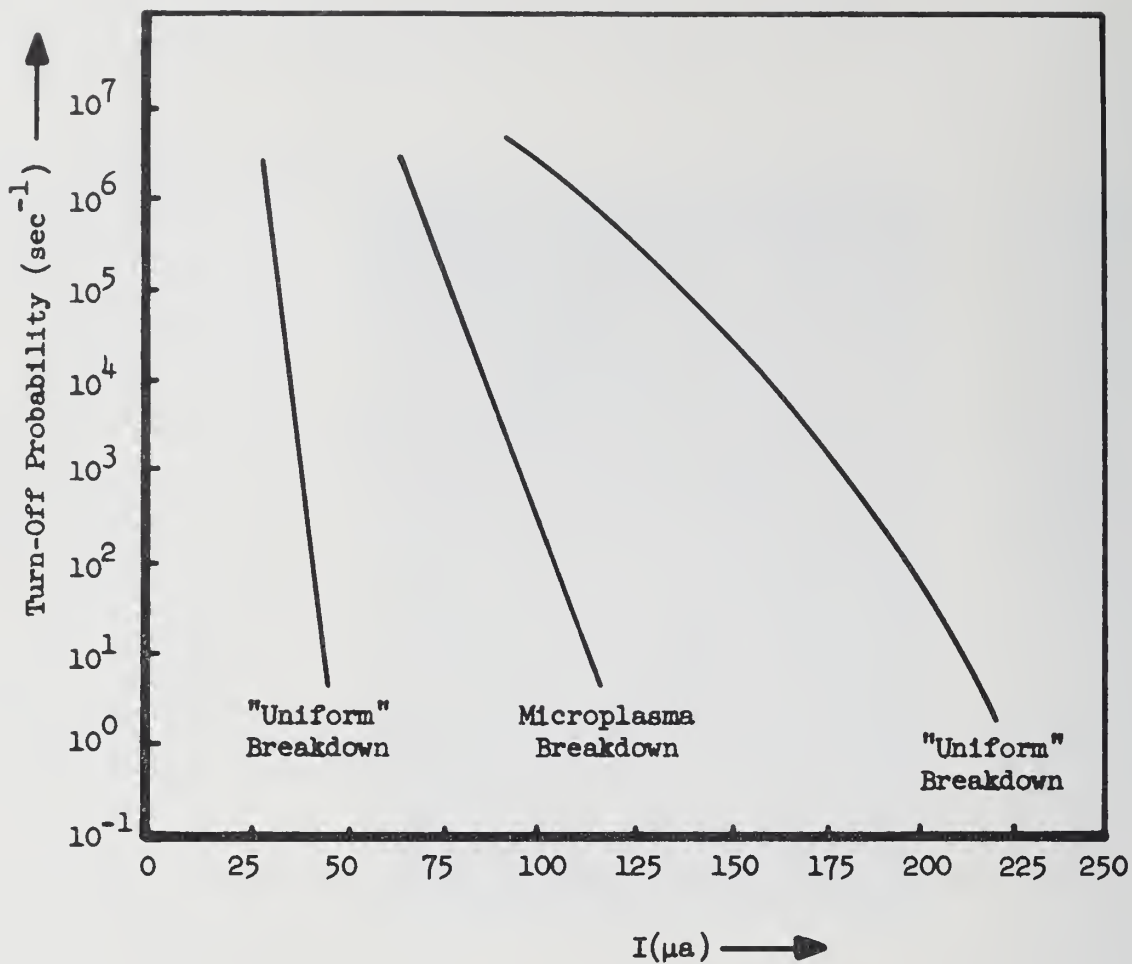


Figure 5. Approximate Turn-Off Probability as Function of Junction Current (Haitz, McIntyre)

McIntyre's idea that ionization probability decreases with increased lattice heating. It seems as if the higher lattice heating increases the lattice scattering cross-section, thus reducing the mean free path and hence the energy gain by the carriers per free path. Tokuyama,²⁰ however, found that breakdown voltages could either increase or decrease with increasing temperature.

McIntyre³ mentioned in his analysis the possibility of extinguishing of the discharge by the decrease in mean free path, but it is evident at closer observation that several further factors may play an important role.

After a discharge has been initiated, both space charge and spreading resistance, as well as compensating recombination tend to stabilize the current.

Jonscher²⁴ writes for the ionization rate

$$\alpha_i n [N_D - (N_A + n)]$$

where

α_i is the ionizing coefficient

$N_D - (N_A + n)$ is the density of ionizable impurities

n is the total density of free carrier

The recombination rate is considered dependent upon three recombination processes viz., recombination accompanied by phonon emission, by photon emission and by Auger (impact) recombination. The first two processes are considered strongly temperature-dependent, increasing sharply as the temperature drops. Among other things this means that although the mean free path decreases with temperature, the number of heat-generating collisions (phonon recombinations) also increases with lowering temperature. It will be evident that with the limited data obtainable from external observations on the integrated effects of all these processes, it will not be profitable to further speculate at this stage.

5.2 Electrical Equivalent Circuit

An electrical equivalent circuit for the process under investigation is a necessity for successful application. The original circuit as proposed

by Rose⁶ is shown in Fig. 6. A description of the breakdown mechanism and subsequent "charge state" of the depletion region leads to a model closely analogous to gaseous breakdown (Fig. 7). A severe shortcoming here, however, is the inherent negative resistance characteristic implied, while there is increasing doubt about the presence of any negative resistance at all.¹⁹

A later model by Champlin,⁸ where the initiating voltage V_B is followed by a voltage interval dV where the breakdown seems unstable and above $(V + dV)$ becomes stable again, has had some success. As pointed out by Haitz, however, this model describes quite well only the behavior in high impedance circuits but fails when the microplasma junction is in a low impedance circuit.

One of the most recent models is that by Haitz¹⁹ with this model containing the largest number of independent parameters viz., extrapolated breakdown voltage V_B (Fig. 8) series resistance R_s , turn-off probability.

It is significant though that although mention has been made²¹ of the possible importance of temperature on the process to be described, it has not explicitly been incorporated in the model. Also, the insistence of many authors on the essential "chance variation" in junction current to explain extinction of the discharge, does not always seem plausible. It is thought that thermal effects play a much more important role than hitherto attributed to them and that in fact, the "on" and "off" characteristic can adequately be described by thermal considerations together with some randomness caused by the trapping and release of carriers in the depletion region. Some observed characteristics are however not explained by the models just mentioned.

First, just "at" the critical applied voltage, the observed breakdown current pulses are not all amplitude limited as predicted but vary widely in amplitude from practically zero to some well-defined maximum--see the top trace in Fig. 9. (This trace, obtained with the same circuit as that on page 3, represents a 1/50 sec exposure of the film.) It seems obvious that in this trace the smaller pulses have a shorter duration than the larger ones.

Depending now upon the role played by temperature, two explanations are possible:

If higher lattice temperature aids the breakdown process it could be argued that a small pulse generates too little heat to keep itself going with the barely sufficient field strength. The larger pulses then obviously are of longer

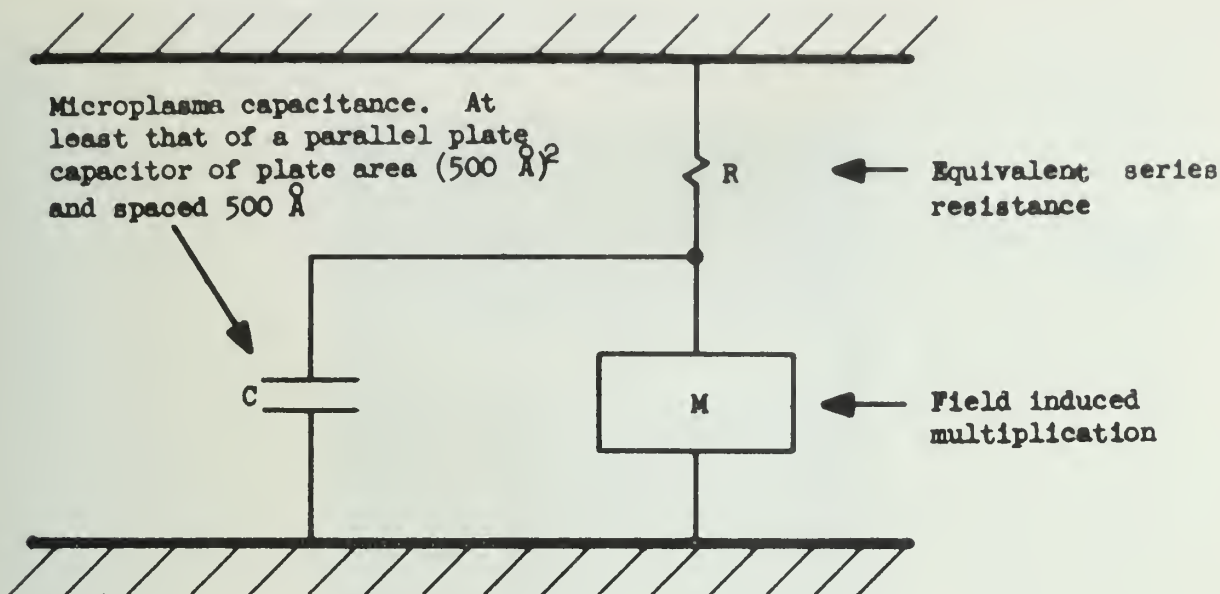


Figure 6. Electrical Equivalent Circuit (Rose)

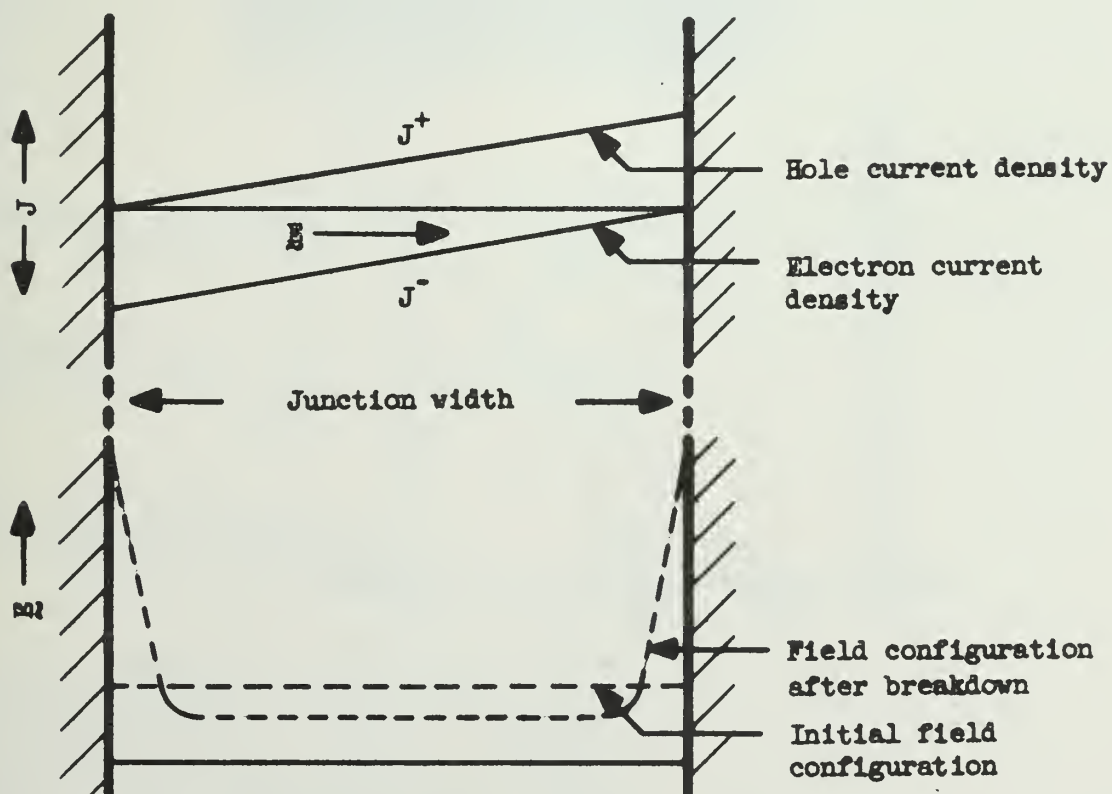


Figure 7. Electrical Model (Rose)

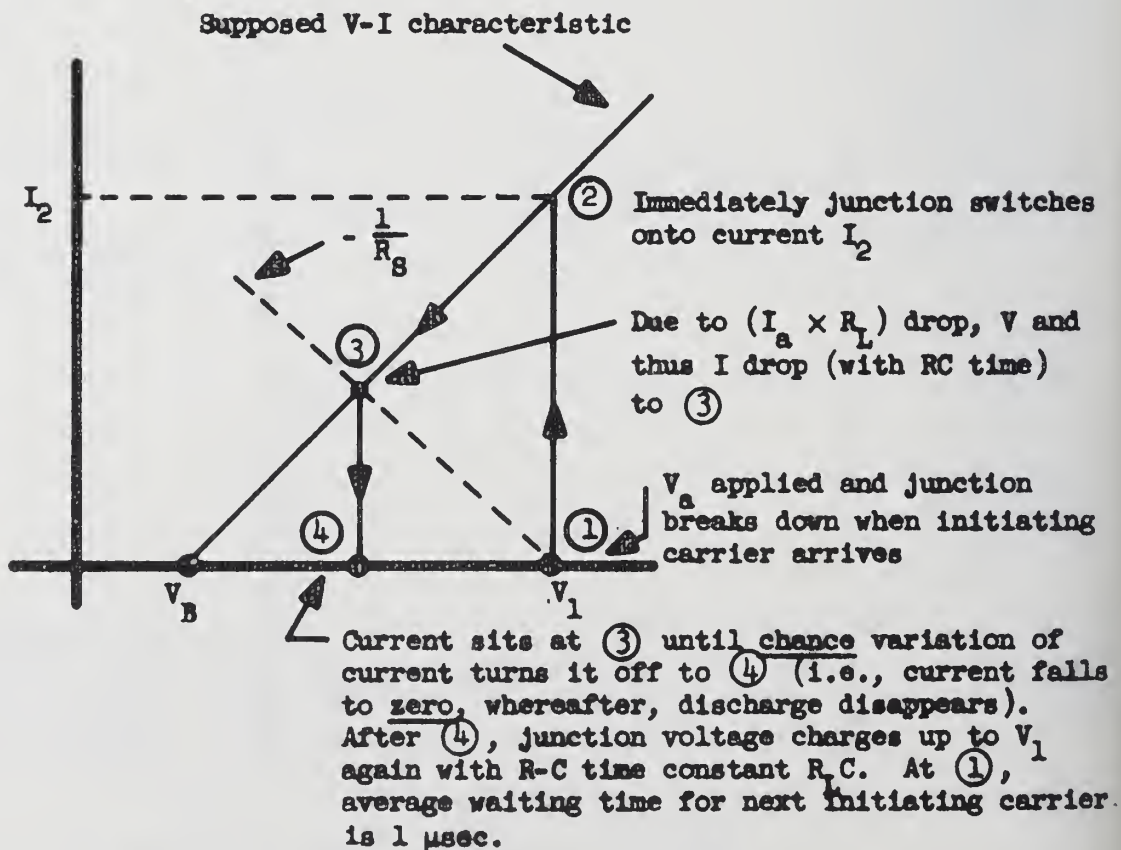
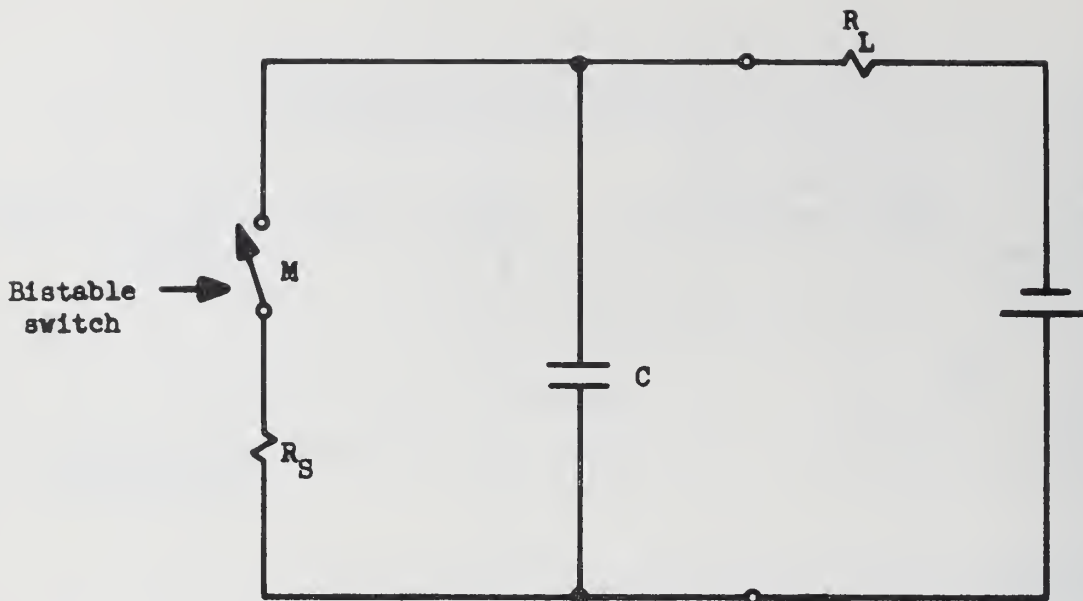
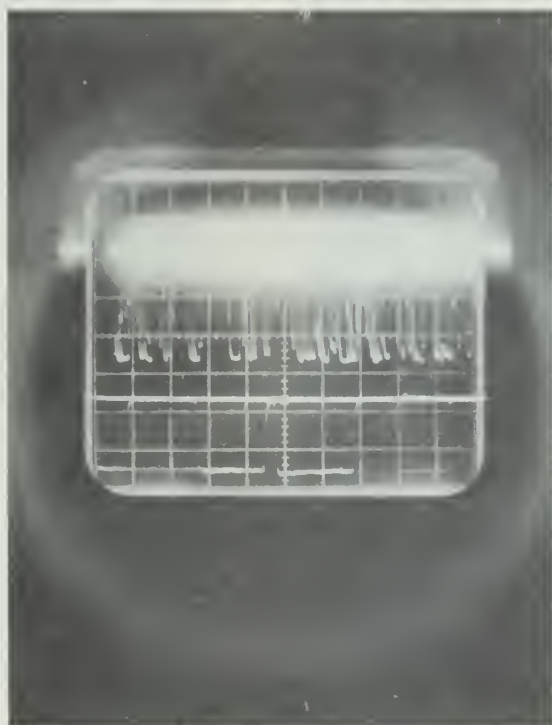


Figure 8. Microplasma Equivalent Circuit (Haitz)



Time base: 10 microsec/cm
Top trace: 50 microamp/cm
Bottom trace: 100 microamp/cm

Figure 9

duration due to greater I^2R losses. This explanation, however, does not give a reason for the "why" of small and large pulses.

A different role for the temperature could lead to the following reasoning: this seems the more plausible explanation since it is readily established that at fixed externally applied voltage, an increase in temperature of a fraction of a degree Kelvin greatly reduces the number of breakdowns per second in a junction.

The argument then is: At a certain instant, at a particular point in the junction, the field is just barely sufficient to start a breakdown and a small current pulse ensues. This pulse is, however, just on the verge of the possible due to the low field, and the least decrease in energy gained from the field--this decrease being the result of shorter mean free path due to larger lattice vibration caused by ohmic losses--causes it to extinguish, very soon after starting. The larger pulses however represent the currents started by field conditions capable of initiating a heavier pulse and thus require more heat to turn them off.

This point of view is further supported by the variation of pulse length with the applied voltage prior to conditions where the field is sufficient to keep the junction continuously on. The lower trace of Fig. 10 shows that an applied voltage about 50 mv higher than that applicable to the upper trace, the pulses are considerably longer and also have much longer periods between pulses. In the light of the foregoing discussion the higher field then initiates a heavy pulse which remains on quite long before enough heat is generated to extinguish it. It is of course true that the larger currents generate much more heat than the smaller currents, considering the squared current relation to the losses; however, as was experimentally observed by several authors, the larger currents also have paths of larger cross-section so that the current flowing and the temperature rise will not be simply related.

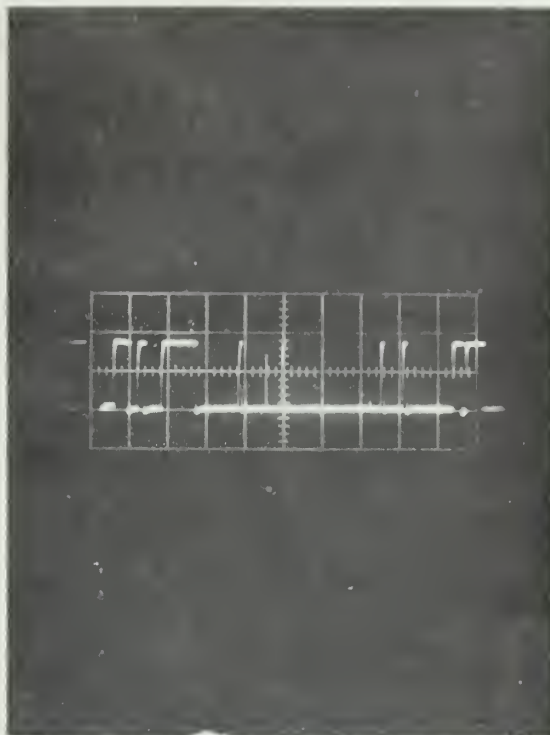
After the heavy pulse has virtually extinguished itself due to the heat it generated, the lattice also takes longer to recover before allowing the next pulse as shown by the longer "dead" times.

It is considered that the possibility of a thermal origin for the switching off of the currents is a much more likely phenomenon than the arbitrary "chance" variation proposed by McIntyre.⁷ Particularly since this chance variation seems to require a momentarily decrease to zero of a current of up to 200 microamp, does its likelihood seem remote.



Short ON-time just at breakdown.

Time base: 100 microsec/cm
Vertical: 100 microamp/cm



Short OFF-time about 50 mv above
initial breakdown.

Time base: 100 microsec/cm
Vertical: 100 microamp/cm

Figure 10

The one unexplained phenomenon of the mechanism proposed above is the reason for varying field conditions giving rise to a tendency for large or small pulses to appear.

Figure 10 gives further evidence of the well known variation of ON-time with applied voltage.

In essence the proposed model would then be the following: At a certain lattice temperature T_1 , a minimum electric field is required in the depletion region to impart sufficient energy for ionization to a carrier entering this high field region with zero velocity. Except possibly at very high temperatures, all carriers entering the depletion region may be considered to have zero velocity compared to their subsequent velocity.

Taking into account the mean free path applicable, such a carrier, entering the depletion region is accelerated by the field and gains energy with time, the rate depending upon the collision rate with the lattice and the corresponding loss of energy to the lattice. This energy loss heats up the lattice, increases the number of collisions by reducing the mean free path and thus also the net energy transfer from field to carrier is reduced; the discharge thus extinguishes. Due to heat conduction the lattice cools down practically immediately, thus creating conditions where the next discharge may start. It is thus seen that in spite of the presence of a sufficiently strong field as well as initiating carriers, the lattice temperature has to be below a certain value for the discharge to start. As soon as it starts it extinguishes itself by increasing the lattice temperature--a type of squelching oscillation may thus be expected, the period being related to the thermal time constant of the junction region.

5.3 Energy Considerations

Before taking a closer look at some detailed experimental observations, it will be in order to make an approximate evaluation of the energy relations mentioned in the paragraphs above.

On page 11, the rate of energy gain from the lattice was given by equation (7) as:

$$\frac{d\epsilon}{dt} = q\mu E^2$$

Now the field in the depletion region will to some extent depend upon the current flowing since resistance will be present in both the diode itself and the supply circuit. It is thus conceivable that the field will drop as the current switches on, and even though the thermal effects may not extinguish the discharge a too low field may also be the cause; this will have to be included in the picture.

If a critical initiating field is assumed as was mentioned above, this field being E_c , the field at any subsequent instant t will be:

$$\left[E_c + \frac{\partial E}{\partial t} t \right]$$

$\left(\frac{\partial E}{\partial t} \right.$ will be negative.) The mean rate of energy gain in the interval t will thus be:

$$\frac{\partial \epsilon}{\partial t} = q\mu \left[E_c + \frac{\partial E}{\partial t} \frac{t}{2} \right]^2 \quad (20)$$

The rate of energy loss to the lattice had been previously found to be:

$$\frac{\partial \epsilon}{\partial t} = \frac{16kT_2 u^2}{\lambda} \sqrt{\frac{m}{2kT_2 \pi}} \left(1 - \frac{T_2}{T_1} \right) \quad (21)$$

As noted before, the effective carrier temperature T_2 may be expressed as a function of the field in the form:

$$T_2 = \frac{T_1}{2} \left[1 + \sqrt{\frac{3\pi}{8} \left(\frac{\mu_0 E}{u} \right)^2} \right] = \frac{T_1}{2} [1 + K_4 E]$$

where

$$K_4 = \sqrt{\frac{3\pi}{8} \left(\frac{\mu_0 E}{u} \right)^2}$$

Equation (21) thus becomes:

$$\left. \frac{\partial \epsilon}{\partial t} \right|_{\text{lattice}} = K_5 \sqrt{\frac{T_1}{2} (1 + K_4 \bar{E})} \left[1 - \frac{1}{2} (1 + K_4 \bar{E}) \right] \quad (22)$$

with

$$K_5 = \frac{16ku^2}{\lambda} \sqrt{\frac{m}{2k\pi}}$$

The rates of energy gain, given by (21) and (22), both multiplied by the time t , will give the total energy gained in the depletion layer. For determining the limits of microplasma formation this may be equated to the required ionization energy.

The complete expression thus becomes:

$$q\mu \left[\bar{E}_c + \frac{\partial \bar{E}}{\partial t} \frac{t}{2} \right]^2 t + K_5 \sqrt{\frac{T_1}{2} (1 + K_4 \bar{E})} \left[1 - \frac{1}{2} (1 + K_4 \bar{E}) \right] t \geq \epsilon_{\min} \quad (23)$$

where

$$K_4 = \frac{3\pi}{8} \left(\frac{\mu_0}{u} \right)^2$$

$$K_5 = \frac{16ku^2}{\lambda} \sqrt{\frac{m}{2k\pi}}$$

In equation (23) $\frac{\partial \bar{E}}{\partial t}$ still has to be found.

5.3.1 Determination of $\frac{\partial \bar{E}}{\partial t}$

Experimental evidence of microplasma behavior (e.g., Fig. 1) shows that the current is amplitude limited. This means that, no matter with what time constant the current rises, it tends to some final value in a very short time. It will be assumed that the rise in current is determined by some time constant τ , and that the current as a function of time may be expressed by the relation

$$I = I_0(1 - e^{-t/\tau})$$

where I_0 is the final value. In the depletion region the field \bar{E} will be given by:

$$\bar{E} = \frac{V - IR}{W}$$

where V is the applied voltage, R the effective series resistance while as before, W is the effective width of the space charge region.

If it is assumed that we have an abrupt junction, as was the case in the units under test, the voltage and space charge width are related by:

$$W \propto \sqrt{V}$$

i.e.,

$$\bar{E} = K_1 \left(\sqrt{V} - \frac{IR}{\sqrt{V}} \right) = K_1 \left[\sqrt{V} - \frac{I_0(1 - e^{-t/\tau})R}{\sqrt{V}} \right]$$

The rate at which \bar{E} changes with time will thus be given by:

$$\frac{\partial \bar{E}}{\partial t} = - \frac{K_1 I_0 R}{\tau \sqrt{V}} e^{-t/\tau} \quad (24)$$

Equation (24) may be used in (23) but the time constant τ still have to be determined.

The microplasma itself has been found by several workers to be about one micron in length, and the total charge in its length will thus be given by:

$$Q = \frac{I \times W}{\bar{v}}$$

and by using previously mentioned values of

$$I = 100 \mu a$$

$$W = 10^{-6} m$$

$$\underline{v} = 0.128 \times 10^7 m/sec$$

$$Q = 10^{-16} coulomb$$

If the voltage across this region is 20 volts, the capacitive effect associated with it is:

$$C = \frac{Q}{V} = 10^{-16} farad$$

With a possible series resistance of 10^4 ohms, the R-C time constant becomes:

$$\tau \simeq 10^{-12} secs$$

This result leaves only t as the unknown in equation (23).

The term $(1 + K_4)$ in (23) may be written as:

$$(K_6 + K_7 e^{-t/\tau})$$

where

$$K_6 = 1 + K_1 K_4 \sqrt{V} - \frac{K_1 K_4 I_0 R}{\sqrt{V}}$$

Filling in the expression for $\frac{\partial \underline{E}}{\partial t}$, (23) becomes:

$$qm \left[\underline{E}_c - K_8 e^{-t/\tau} \right]^2 \cdot t + (K_9 - K_{10} e^{-t/\tau}) \sqrt{K_{11} + K_{12} e^{-t/\tau}} \cdot t \geq \epsilon_{min} \quad (25)$$

with the constants being given by:

$$K_1 = \frac{\sqrt{V}}{W}$$

$$K_9 = \left(1 - \frac{K_6}{2}\right) K_5$$

$$K_4 = \sqrt{\frac{3\pi}{8} \left(\frac{\mu_0}{u}\right)^2}$$

$$K_{10} = -\frac{1}{2} K_5 K_7$$

$$K_5 = \frac{16ku^2}{\lambda} \sqrt{\frac{m}{2k\pi}}$$

$$K_{11} = \frac{T_1}{2} K_6$$

$$K_7 = \frac{K_1 K_4 I_0 R}{2\tau \sqrt{V}}$$

$$K_{12} = \frac{T_1}{2} K_7$$

$$K_8 = \frac{K_1 I_0 R}{2\tau \sqrt{V}}$$

From equation (25) it will now be possible to find

$$t = f(I_0)$$

assuming all the other parameters to be constants. It might also be more appropriate to write up a computer program for finding t as a function of several of the parameters likely to vary, like temperature. This is quite feasible at the present stage, but it is felt that quite considerably more experimental data of the microplasma type behavior should be gathered so as to act as guide lines in making approximations and thus evolving more practical equations.

At this stage some remarks about the energy required for ionization and the process itself are in order.

The true ionization energy required is not a readily determinable quantity. As mentioned by Jonscher²⁵ the mean value theory has to some extent explained experimental results. This theory requires that the critical breakdown field is only reached when the average energy of all carriers present reaches a certain fraction, γ , of the "true" ionization energy-- γ has been found to be of the order of 0.2.

It seems though that the above reasoning points to a weak link in the efforts to reconcile theory and experiment in the case of breakdown phenomena.

It is suggested that the value 0.2 is just a result of the fact that only at this value of γ are there sufficient carriers at ionizing energies to make their influence observable. Limitations of oscilloscopes and related equipment has very often been found to be the determining factor in deciding upon threshold values for breakdown voltages. Extremely accurate experimental observations over a considerable period of time on several samples support the view that often some extent of breakdown already is present before the positively identified discharge is noted. This point was also commented on by McIntyre⁷ and is further illustrated by the fact that as ever better junctions are produced, the equivalent circuit seems to be getting ever simpler.

In order to obtain some idea of how the energy conditions of the carriers in the depletion region would change with time, the equation giving the energy gained and lost may be further examined.

5.4 Energy Gained

The first term of equation (25) gives the energy gained by the carriers from the electric field E , in the depletion region.

The rate of energy gain with time was originally given as

$$q\mu E^2$$

so the total energy gained in time will be a function of both the field and of the time, say Δt , itself.

Considering for the moment interpretation of the time, Δt : If at instant $t = t_0$ one has $T = T_0$ and $E_0 > E_c$ where E_c is the minimum field to cause ionization at temperature T_0 , the time Δt will indicate how long the breakdown may remain on. It is explicitly stated that it may remain on for Δt , since there is no guaranty that the breakdown will start as soon as the voltage is applied; at the end of Δt though, the breakdown will cease. Trapping of course may also play a part in the behavior as has already been mentioned.

Consider now the terms representing energy gained:

$$q\mu[E_0 - E(t)]^2 \cdot \Delta t$$

The component $E(t)$ of the field which varies with time is a result of the current varying with time. (A second order effect, due to variation in W will be neglected.)

Since the current starts at zero, this field component should start at zero and after infinite time will be equal to

$$\frac{I_0 \cdot R}{W}$$

Thus:

$$E(t) = \frac{I_0(1 - e^{-t/\tau})R}{W}$$

and the energy gained in time Δt may be expressed by

$$q \cdot \mu \left[E_0 - \frac{I_0 R}{W} (1 - e^{-t/\tau}) \right]^2 \cdot \Delta t$$

if Δt is small. Using some of the values given in the Appendix, and considering Δt to vary between 0.1τ and 5τ , Fig. 11 shows how the energy gained will vary with time. It is important also to note how the rate of energy gain changes with time, as given by the changing slope of this curve, the rate being seen to increase.

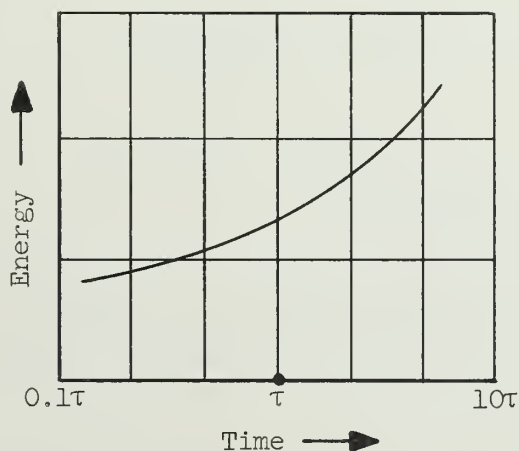


Figure 11. Carrier Energy Gain from Electric Field

5.5 Energy Lost to Lattice

The rate of energy gain from the lattice was given as

$$\frac{\partial \epsilon}{\partial t} = \frac{16ku^2}{\lambda} T_2 \sqrt{\frac{m}{2kT_2\pi}} \left(1 - \frac{T_2}{T_1} \right)$$

and the carrier temperature T_2 , expressed in terms of the lattice temperature as

$$T_2 = \frac{T_1}{2} \left[1 + \sqrt{\frac{3\pi}{8} \left(\frac{\mu_0 E}{u} \right)^2} \right]$$

Substituting for T_2 and grouping terms one may write:

$$\frac{\partial \epsilon}{\partial t} = \frac{K_5}{2\sqrt{2}} \sqrt{T_1(1 + K_4 E)} (1 - K_4 E)$$

where

$$K_4 = \sqrt{\frac{3\pi}{8} \left(\frac{\mu_0}{u} \right)^2}$$

$$K_5 = \frac{16ku^2}{\lambda} \sqrt{\frac{m}{k\pi}}$$

In this expression both E and T_1 will be functions of time so that also the rate of energy loss is going to vary with time.

5.5.1 Variation of T_1 with Time

Rose⁶ has analyzed the heat distribution inside a probable model of a microplasma region, and by taking account of heat loss to the surroundings, he finds that at a dissipation rate P joules/sec, the temperature increase will be:

$$\Delta T = \frac{3\Gamma(\frac{3}{2})P}{4\pi \frac{3}{2}k}$$

where

k is the heat conductivity in j/sec cm °C

and

ℓ is the diameter of a sphere in which the dissipation is assumed to take place

Since

$$P = I^2 \cdot R = I_0^2 R (1 - e^{-t/\tau})^2$$

the temperature of the microplasma region, which is given by:

$$T_1 = T_0 + \Delta T$$

will vary with time, increasing to a final value determined by $I_0^2 \cdot R$.

As shown by the expression for ΔT , this temperature rise will not be a simple function of the dissipation, and as an approximation it will simply be written as:

$$\Delta T = K_T I_0^2 (1 - e^{-t/\tau})$$

where K_T is some constant. The lattice temperature T_1 should thus be replaced by

$$T_1(t) = T_0 + K_T I_0^2 (1 - e^{-t/\tau})^2$$

5.6 Complete Expression for $\frac{\partial \epsilon}{\partial t}$

Incorporating the expression for $T_1(t)$ and $E(t)$ in the expression for the energy gained by the carriers, yields:

$$\begin{aligned} \frac{\partial \epsilon}{\partial t} = & \frac{K_5}{2\sqrt{2}} \sqrt{T_0 + K_T I_0^2 (1 - e^{-t/\tau})^2} \sqrt{1 + K_4 \left[E_0 - \frac{I_0(1 - e^{-t/\tau})R}{W} \right]} \\ & \times \left\{ 1 - K_4 \left[E_0 - \frac{I_0 R}{W} (1 - e^{-t/\tau}) \right] \right\} \end{aligned}$$

This rate of energy exchange may be evaluated at a few points, such as shown below:

$$\text{At } t = 0: \quad \frac{\partial \epsilon}{\partial t} = \frac{K_5}{2\sqrt{2}} \sqrt{T_0} \sqrt{1 + K_4 E_0} (1 - K_4 E_0)$$

$$\text{At } t = \tau: \quad \frac{\partial \epsilon}{\partial t} \approx \frac{K_5}{2\sqrt{2}} \sqrt{T_0 + 0.14 K_T I_0^2} \sqrt{1 + K_4 \left[E_0 - \frac{0.4 I_0 R}{W} \right]} \times \left[1 - K_4 \left(E_0 - 0.4 \frac{I_0 R}{W} \right) \right]$$

$$\text{when } t \rightarrow \infty: \quad \frac{\partial \epsilon}{\partial t} \rightarrow \frac{K_5}{2\sqrt{2}} \sqrt{T_0 + K_T I_0^2} \sqrt{1 + K_4 \left[E_0 - \frac{I_0 R}{W} \right]} \left\{ 1 - K_4 \left[E_0 - \frac{I_0 R}{W} \right] \right\}$$

Inspection of the above expression shows that the rate of energy exchange decreases with time, and furthermore is of such a sign as to indicate energy transfer from carrier to lattice. This agrees with the fact that at the fields under consideration the effective temperature of the carriers will be much higher than that of the lattice.

Sketching out the variations in $\left(\frac{\partial \epsilon}{\partial t}\right)$ with time as arrived at above, for both the energy gained from the field and that lost to the lattice, some interesting points come to light.

Consider first Fig. 12 where on the same axes is shown the variation in energy gained and energy lost by the carriers-- the rate of energy gained is seen to increase with time, while the rate of energy lost decreases with time.

It is tacitly assumed in this first case that the energy gained is more than the energy lost at $t = 0$.

The net gain in energy by the carriers will be given by the difference between the ordinates of the curves--this difference is plotted in Fig. 12.

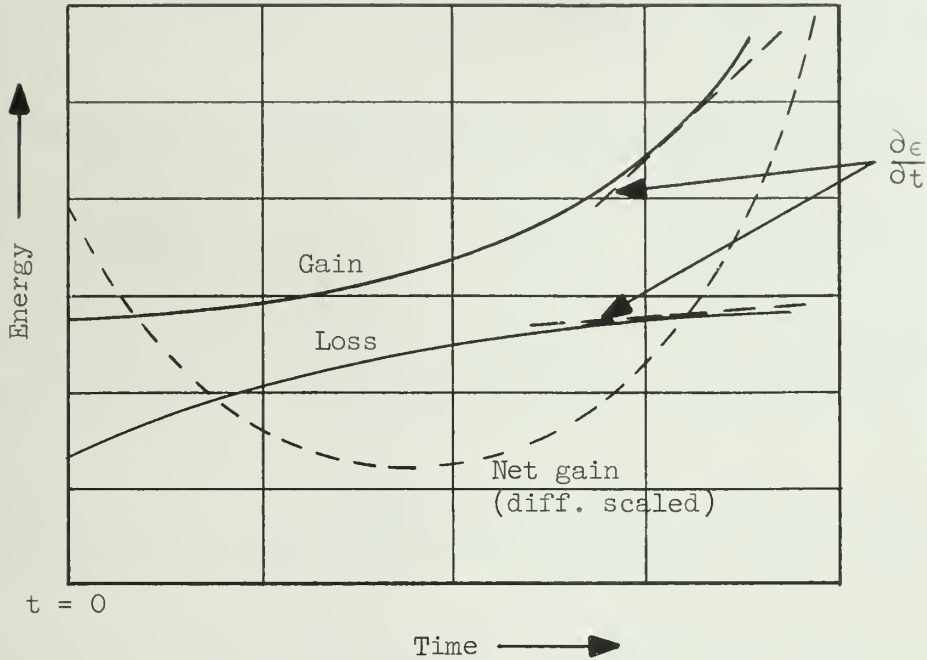


Figure 12. Carrier Energy Gain and Loss

Depending now on the value of the minimum required ionization energy, different conditions in the depletion region may prevail. Consider Fig. 13 where the dotted lines indicate different values of the difference between energy gained and lost--this latter difference will have an absolute value determined by applied voltage, initial temperature, etc.

The value, ϵ_i , indicated below is the minimum required ionization energy, its value depending among other things upon the material being used.

Curve A indicates the case where the applied field would be too weak to cause any ionization at all during the time the carrier spends in the high field region.

Consider then Curve B: If the applied voltage is so high as to give ϵ_b as the initial net energy gain, ionization will result, and the microplasma will switch on. It will then remain on until time t_b when the net gain in

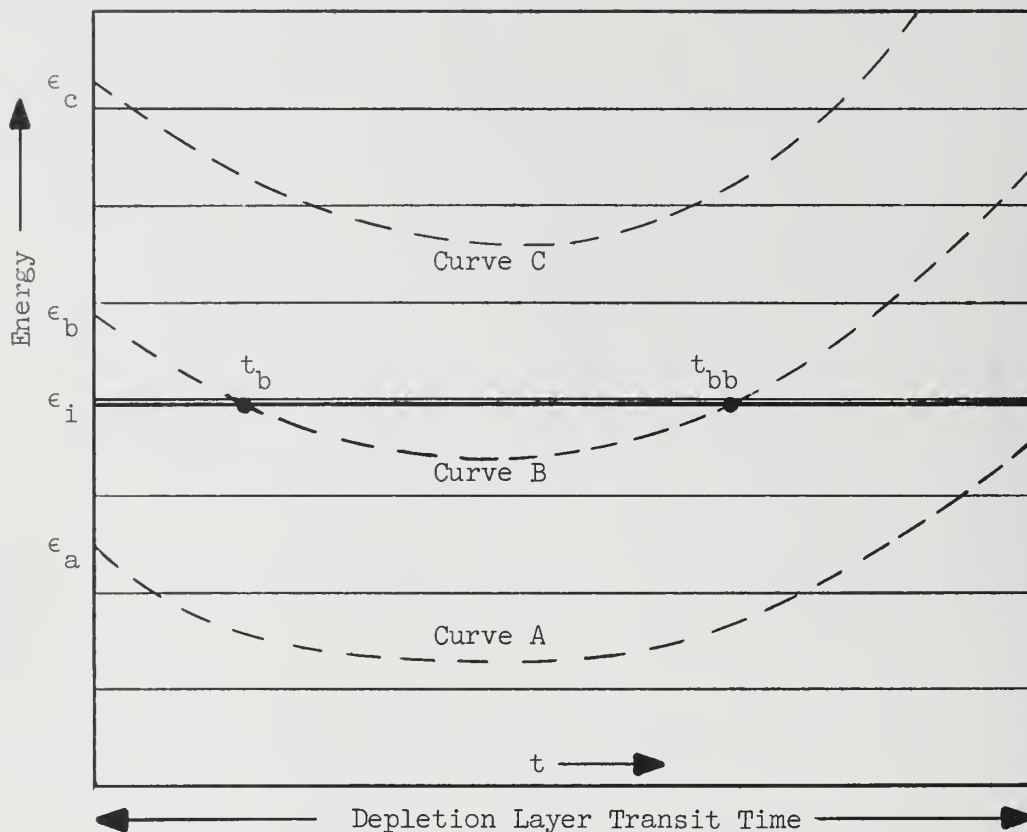


Figure 13. Varying Conditions in the Depletion Region

energy will fall below the required ionization value and the discharge should extinguish. However, at time t_{bb} the energy gained will exceed the energy lost by a sufficient amount to re-ignite the discharge.

Curve C will represent the case where the applied voltage is so large that at no time during transit of the depletion region does the energy fall low enough to extinguish the discharge.

Apart from any trapping effects it will be obvious that a certain randomness will be introduced by the energy with which a carrier enters the depletion region.

Apart from statistical considerations, a very detailed observation of delay times and pulse lengths as functions of applied voltage will have to be made to provide experimental proof for the arguments above.

In Fig. 14 below are shown some current pulse distributions in time, as would result from differing initial energies for carriers entering the high field region.

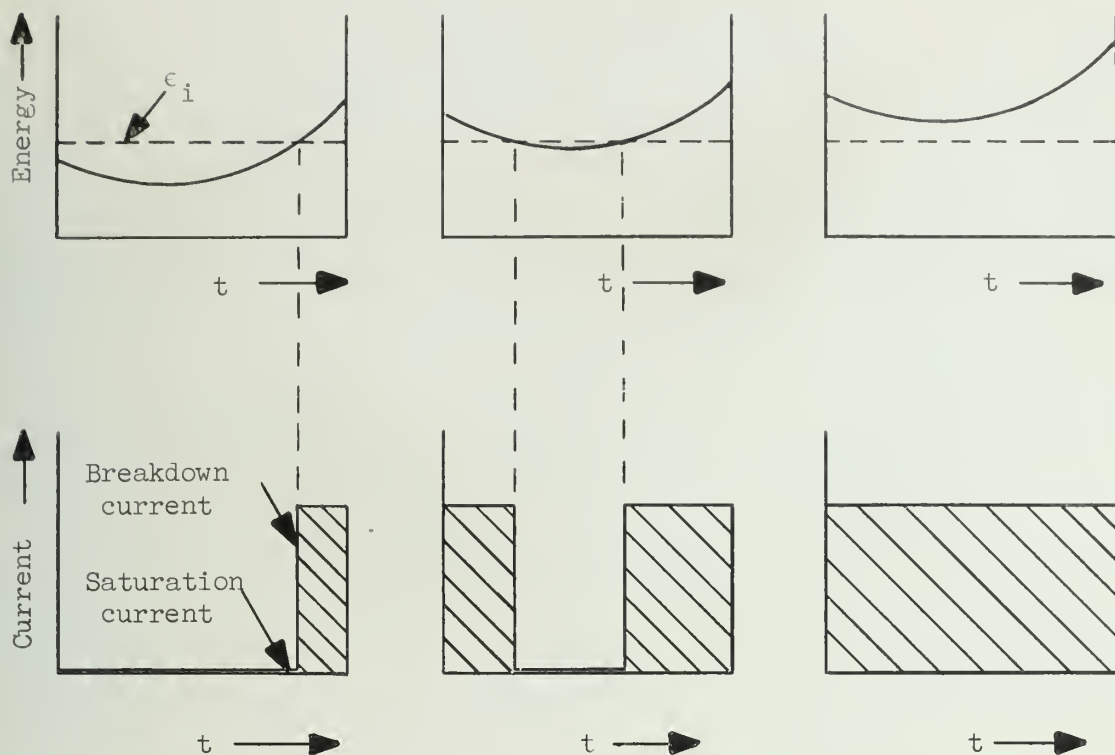


Figure 14. Current Pulse Distributions in Time

It is conceivable that, instead of the initial conditions being greater gain than loss in energy, it could be the other way round. This means that a carrier entering the depletion region would for the first short time interval lose more energy to the lattice than it was gaining from the electric field. Due however to the increase in rate of energy transfer from the field accompanied by the decrease in the rate of loss to the lattice, the carrier can still exceed the critical energy while in transit across the high field region.

In this case, the curves of Fig. 15 would apply, they being analogous to those of Fig. 13.

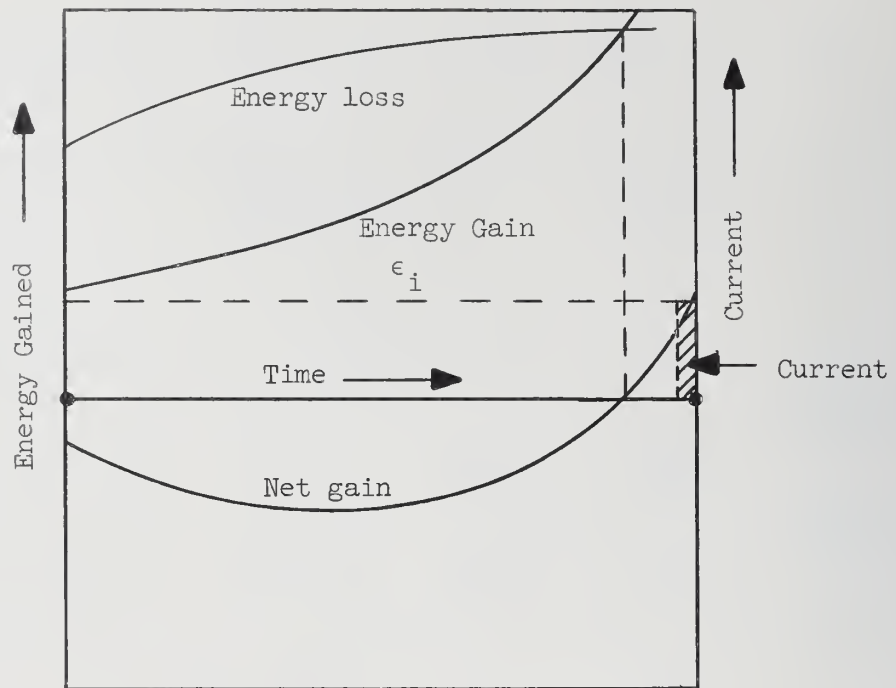


Figure 15. Alternative Condition for Carrier Energy Gain and Loss

6. MICROPLASMA CHARACTERISTICS

6.1 General Behavior

Equation (25) illustrates quite adequately that an accurate theoretical description of microplasma breakdown does not seem quite possible as yet. Many constants required for quantitative analysis are completely unknown, so that at best, a semi-empirical solution will be available.

One of the unsolved problems has always been the true shape in time of the microplasma current pulse--the time order discussed in paragraph 2.4 illustrates why experimental measurements are very difficult indeed.

In the sections following some breakdown characteristics of microplasma-type silicon diodes are shown. These diodes, of especially accurate construction, were produced for noise production by the Shockley Laboratories of the Clevite Company and generously donated for the present investigation.

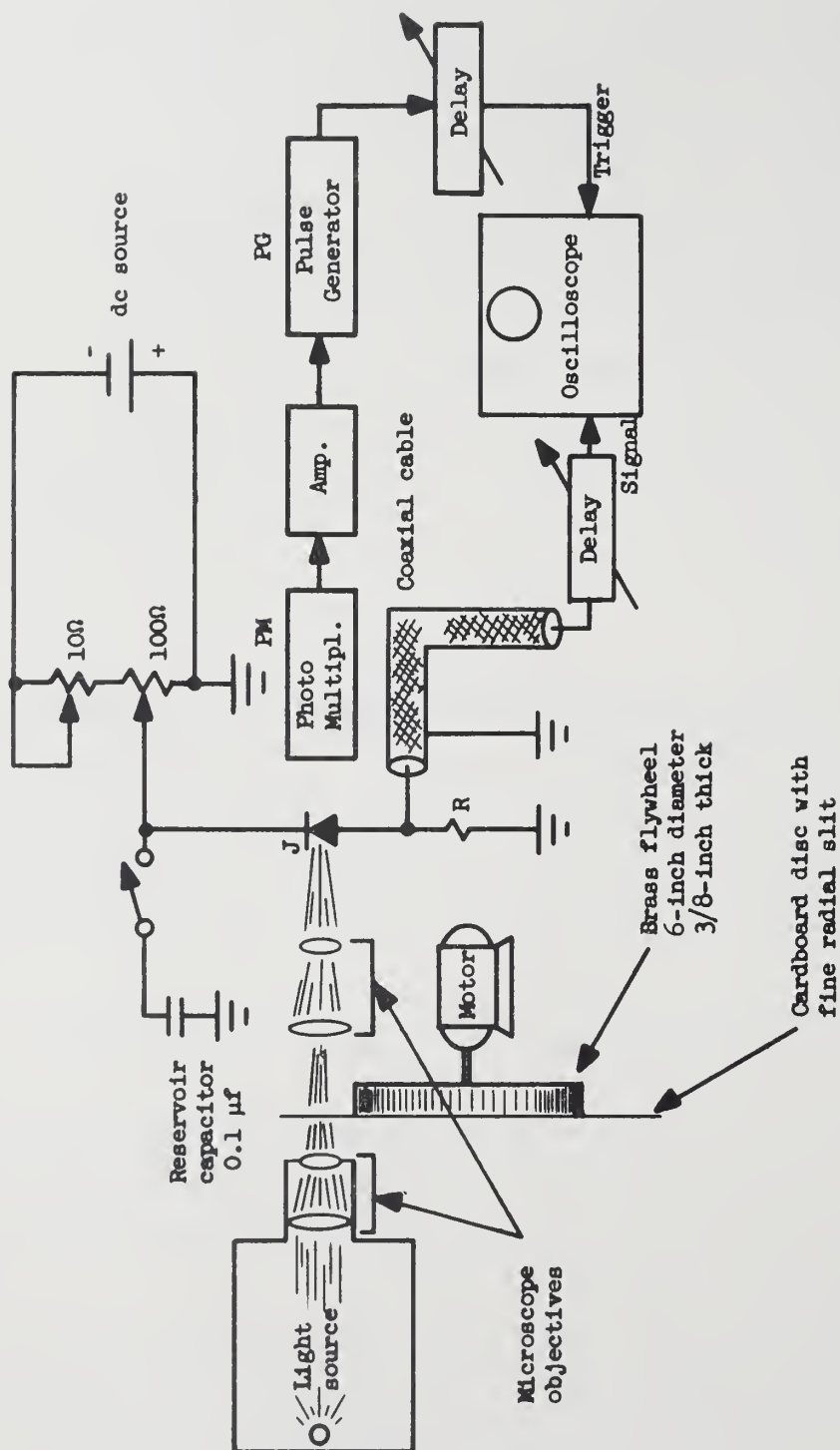
6.2 Experimental Set-Up

Several workers have found that junction breakdown may be precipitated in a junction (where a near-critical field is present) by the injection of photons from outside. It was thus decided to stress a junction electrically with a steady dc field to near its breakdown value and then to inject a periodic light pulse to start the breakdown and give a recurrent microplasma coincidental with the light pulse.

The sketch in Fig. 16 on the next page gives an outlined of the experimental set-up.

The light source is a P.E.K. 109 high-pressure dc mercury arc lamp producing a 0.012-inch cube arc, of 100 watts dissipation. The revolving disc of opaque cardboard was attached to a 6-inch diameter brass flywheel, driven by a 1/16 hp ac-dc Bodine motor at speeds up to 6000 rpm.

The light from the source is first focused onto a fine slit in the disc; thereafter it is again focused onto the junction at J. Some light spills past the junction and is picked up by the photomultiplier PM which delivers, via a three-stage amplifier, a trigger pulse for the pulse generator PG. This pulse generator was then employed to give a trigger pulse for the oscilloscope.



Light source: P.E.K. 109 high-pressure mercury arc, 100 watt, fan cooled.

Pulse generator: Datapulse model 102.

Motor: Bodine ac-dc type N.S.E.-13, 1/16 hp, 115 volt.

Oscilloscope: 516A with any of the following plug-in units:

3A1 dual trace amplifier (10 mc/sec)

2A63 differential amplifier (0.3 mc/sec)

2B67 time base

Figure 16. Experimental Set-Up

The actual voltage pulse from the pulses of microplasma current is taken across the resistor R in series with the diode.

6.3 First Experimental Results

In Fig. 17 on the next page are shown some oscillographs of microplasma breakdowns.

Photo (a), which was taken at room temperature, shows that although microplasma pulses are present all the time once the potential has reached a certain value, many more breakdowns are produced when the high pulse reaches the junction; this would indicate that photons aid in the production of ionized regions.

It is significant though that although a steady stream of photons reaches the junction while the light pulse is on, the breakdown is not continuous--this is clearly seen in the close-up of photos (b) and (c).

It is possible however to eliminate spurious breakdown between light pulses by shielding the junction from ambient light and cooling to liquid nitrogen temperature. Fig. 19 on page 55 shows clearly that between light pulses no other breakdowns are present or that they are at least so weak or fast as to be not observable on the oscilloscope in spite of the long exposure (3 secs) used for photo.

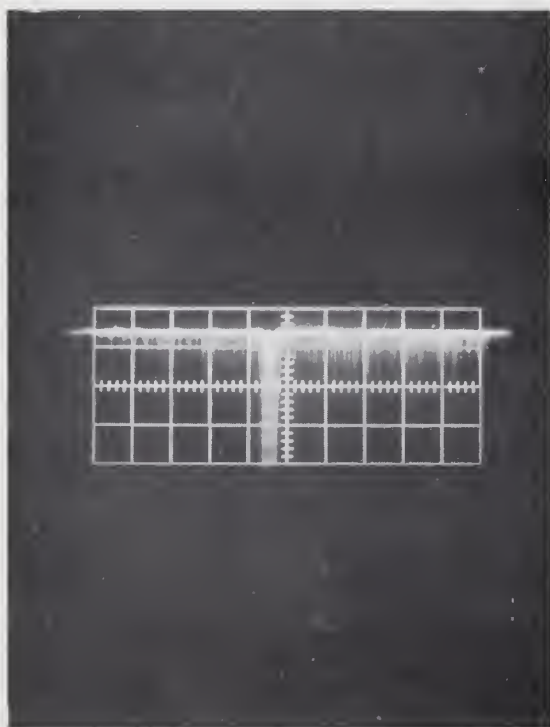
All the evidence cited above indicates that thermal influences play a major role in the formation of microplasma breakdowns, as had been mentioned during the foregoing analysis.

A further significant point is that as is indicated in Figs. 18a and 18b the ruling temperature certainly influences the rise and fall times of the current pulses. Figure 18 shows that although the rise time is sharp, at room temperature, the pulse dissipation increases the ambient temperature and when due to this rise in lattice temperature the breakdown extinguishes, there follows a relatively long fall time. At liquid nitrogen temperature Fig. 18 indicates that when the lattice is continually cooled, the fall time approaches that of the rise time.

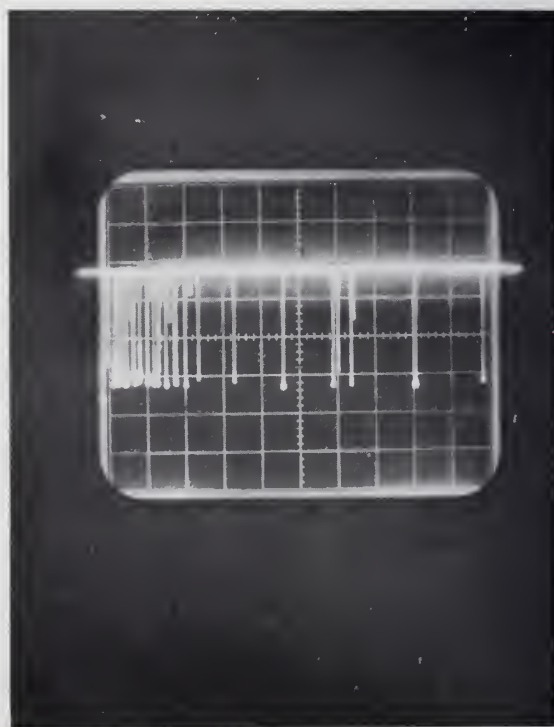
In an attempt to find the true pulse rise time, it will be obvious that the conventional oscilloscopes employed above are much too slow, considering the expected rise times of picoseconds.



(a) Time base: 5 msec/cm
Vertical: 100 μ a/cm
(exposure time 3 secs)

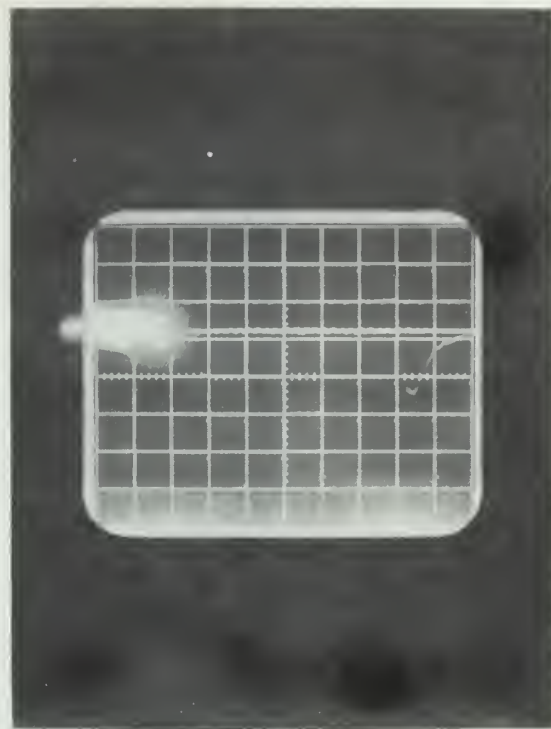


(b) Time base: 50 μ sec/cm
Vertical: 500 μ a/cm



(c) Time base: 5 μ sec/cm
Vertical: 100 μ a/cm

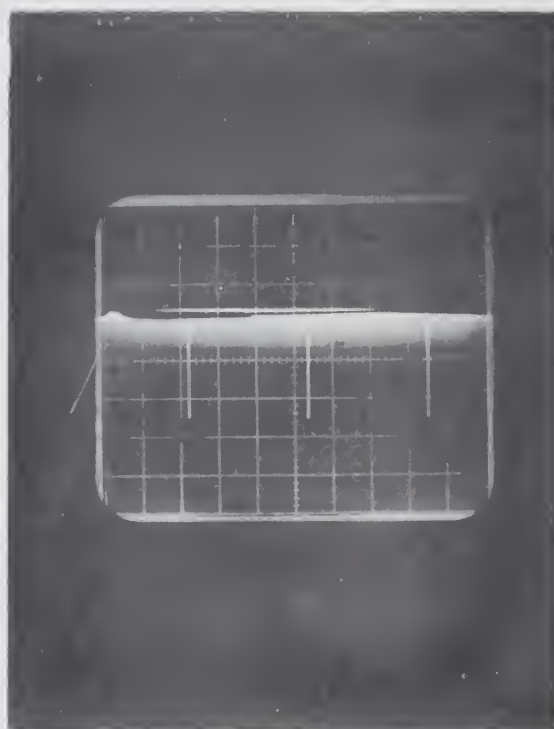
Figure 17



(a) Time base: $2 \mu\text{sec}/\text{cm}$
 Vertical: $500 \mu\text{A}/\text{cm}$ across $1 \text{ K}\Omega$
 (Oscilloscope passband $100 \text{ mc}/\text{cm}$)
 300°K temperature

(b) Time base: $200 \text{ nsec}/\text{cm}$
 Vertical: $100 \mu\text{A}/\text{cm}$ across 100Ω
 (Oscilloscope passband $10 \text{ mc}/\text{sec}$)
 Liquid nitrogen temperature

Figure 18. Influence of Temperature on Rise and Fall Times



Horizontal: 5 msec/cm
 Vertical: 50 μ a/cm
 (exposure time 1 sec)

Figure 19

The only truly fast conventional oscilloscopes are those like the Tektronix 519 with a 1000 mc/sec passband--however, since, this type of 'scope employs a travelling wave type CRT and in order to obtain the mentioned response cannot incorporate any amplifiers, the low sensitivity is prohibitive. Considering that the 519 had a sensitivity of 10 volt/cm and a microplasma pulse has a typical current of 100 microamp, a 10 kilo-ohm resistance is required in series with the diode to provide a vertical deflection of 1 millimeter on the screen. This high value of resistance, together with the stray and input capacitance of the oscilloscope immediately limit the current pulse rise time to something of the order of a nanosecond or more, thus defeating the purpose of the fast oscilloscope. On the other hand, using the 125-ohm input impedance of the 519 as a diode load produces a deflection too small to be detectable--considerable effort was directed at this latter method, hoping to photograph a small deflection and then use photographic enlarging for greater detail. Although the 519 has a very fine trace, no success was achieved with this method.

The only other alternative at the present time is the use of a sampling oscilloscope. In order to do this, the signal to be sampled must, with present-day sampling oscilloscope like the Tektronix 661 or the 3S76 and 3T77 plug-in units for the 561A be of a strictly periodic nature. In the case of microplasmas, it is obvious from Fig. 17a that this will not be an easy requirement to comply with.

The photon bombardment, showing the increased breakdowns in Fig. 17c suggests however that this method might be used to provide a periodic pulse.

6.4 Attempts at Using Sampling Techniques

The circuit used was essentially of Fig. 16 but the oscilloscopes used were, first, a Tektronix 661 with a 4S1 sampling head and a 5T1 timing unit. The current measuring resistance R was eliminated since the 50-ohm input impedance of the sampling unit served this purpose.

Variable delays were available in both the trigger and signal circuits but despite extensive efforts it was not possible to obtain a reliable trace of a single breakdown pulse. Figures 20a and 20b show photographs of sampling 'scope traces. These traces show up some interesting phenomena, even though they do not reflect the true current pulse shape.



(a)



(b)

Figure 20. Sampling Oscilloscope Traces

The following should be stressed at the outset: in displaying the traces of Fig. 20 the sampling oscilloscope was being triggered by the chopped light signal via the photomultiplier and amplifier. The rotating disc caused this triggering signal to have about a 10-millisecond pulse spacing, so that each dot on the trace is separated in real time by this period. Furthermore, the three traces were taken at about one-minute intervals. It is thus remarkable that there is such a correspondence between the traces indicating a definite pattern in the breakdown current waveshape. This may suggest that, despite the present failure, periodic pulses may be produced in these junctions.

The traces show a definite sequence of three breakdowns after which it seems that there is a slow decrease in pulse amplitude before the pulses decrease altogether, to restart the cycle.

6.5 Delay in Switch-On after Simulation

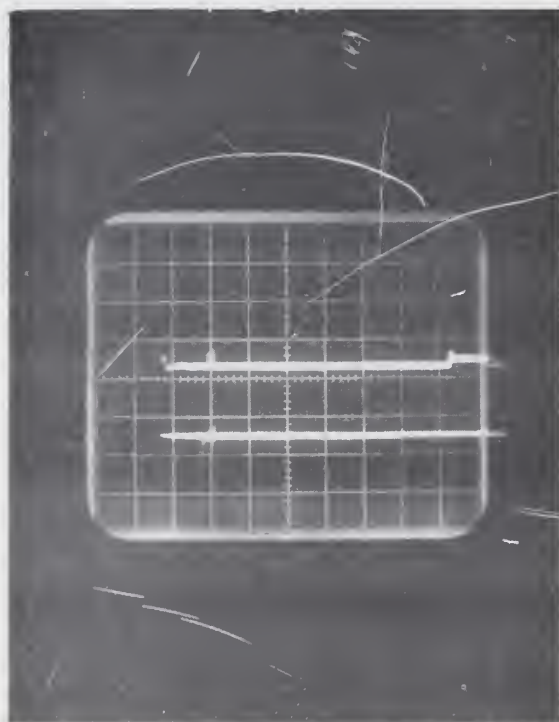
It was mentioned in paragraph 5 that Champlin had found in his work that an average waiting time of one microsecond elapsed after application of the breakdown voltage, before the first microplasma appeared.

When considered in detail, this is not an easily determinable quantity, for several reasons. First, if the applied voltage is slowly increased either smoothly or in steps to the point where breakdowns are evident, it is practically impossible to say at what point the first pulse appeared since a definite change in junction characteristics with time is present. If the junction is electrically stressed for several minutes to just below "breakdown," and the voltage is then increased, this effect is somewhat smaller, but it has not been possible to give a quantitative result in this respect.

If pulsed voltages are used, as was discussed in DCL Report No. 149 these same long time constant effects as well as capacitive surge currents obscure the results. Also, if a nearly large enough dc bias is applied, and a small pulse is superimposed, the condition is improved but suffer from the same disadvantages. At these low levels it must be remembered that where these fast pulses are concerned, matching problems become severe. The microplasma current is only of the order of 100 microamp and in order to prevent circuit RC times from swamping the phenomenon under test, the series resistance for current measurement must be low--say 100 ohms. This means a signal voltage of 10 mv only is available which means that observation is confined to slow oscilloscopes.

Last, but by no means least, come the limitations of the junctions under test. These junctions, as often mentioned, change their response slowly (on the present microsecond time scale) and react differently to dc potentials and to pulses. The present junctions, constructed extremely carefully and from the purest material available, show much less change than the transistors of Report No. 149 but still render impossible the time delay measurement.

Figure 21 below shows breakdowns occurring about 400 to 800 nanosec after application of the pulse--for the present junctions this is a representative figure although both shorter and longer times were observed.



Horizontal: 400 nsec/cm
Vertical: (bottom trace) 100 μ a/cm

Figure 21

7. CONCLUSION

The very fast current pulses produced by high electric field breakdown in Si p-n junctions have been recorded oscillographically. Pulses of hundreds of nanoseconds are easily observed, and are in the 100 to 200 microamp range. Faster pulses of comparable magnitude are visible but it has not been possible to record an individual fast (nanosec or less) pulse, probably due to the still random occurrence.

All lengths of pulses seem available, from spikes too short to be reliably observed on a 5 nanosec rise time oscilloscope (Tektronix 585) to pulses of millisec length--pulse length is smoothly variable by variation of applied voltage. The voltage range effecting this large variation in pulse length varies between diode samples but is of the order of tens of millivolts.

Highly increased pulse repetition rate occurs under photon bombardment from a mercury arc source.

It has not been possible to determine the delay between the application of the light pulse and the appearance of the first discharge--this was due in part to the relatively slow rise time (5 microsec) of the light pulse and the fact that it is not known how much external light is needed to precipitate a breakdown. (Commercially available fast light pulses produce about 2×10^4 photons per 2 nanosec pulse, which after practical experience with the mercury source, is considered too weak. This undoubtedly is due partly to the fact that these diodes under test were encapsulated in glass, making focusing on the diode wafer very difficult.)

Consideration of the breakdown mechanism, as well as detailed experimental observation, suggests that the dominant parameters for breakdown are twofold:

Electric field strength

Lattice temperature

It is believed that all other parameters can be expressed in terms of these two and it is felt that the prime target of microplasma research should be directed at reducing the number of parameters used to describe junction behavior to the above two.

It is believed that positive control over breakdown pulses will become possible in the near future when even better p-n junctions become available.

The easy control over average pulse duration holds promise in fast logic circuits as suggested by Professor W. J. Poppelbaum.

Suggestions for Next Steps in Research

Theoretical: Express turn-on and turn-off probabilities as functions of lattice and of carrier temperature.

Experimental: Obtain junctions not encapsulated and with ample optical access to both sides of the junction. These should preferably be Si structures since Ge is much more opaque to readily available light sources.

Construct dc source of utmost stability and resetability with "zero" internal impedance. Available voltage should be about 40 volts.

Repeat experiments described in this report but with better controlled environment as regards light and heat.

8. APPENDIX

Evaluation of Integrals

Equation (5) read:

$$\frac{d\epsilon}{dt} = A \frac{\int_0^{\infty} (\tilde{y}^3 e^{-B\tilde{y}^2} - C\tilde{y}^5 e^{-B\tilde{y}^2}) d\tilde{y}}{\int_0^{\infty} \tilde{y}^2 \cdot e^{-B\tilde{y}^2} d\tilde{y}}$$

Consider the integral

$$\int_0^{\infty} \tilde{y}^3 e^{-B\tilde{y}^2} d\tilde{y}$$

Let

$$\tilde{y}^2 = x$$

$$2\tilde{y} \cdot d\tilde{y} = dx$$

$$\therefore d\tilde{y} = \frac{dx}{2\tilde{y}}$$

Therefore,

$$\text{Integral} = \frac{1}{2} \int_0^{\infty} x \cdot e^{-Bx} dx$$

The solution to this integral is

$$\frac{1}{2} \frac{\Gamma(n+1)}{B^{n+1}} = \frac{1}{2B^2}$$

with $n = 1$. (C.R.C. Standard Math Tables, C.R.C. Publishing Co., 1962.)

By a similar change of variable the second integral may be evaluated

$$\text{Integral} = \frac{C}{2} \int_0^{\infty} x^2 \cdot e^{-Bx} dx = \frac{C}{2} \frac{n!}{B^{n+1}} = \frac{C}{B^3} \text{ when } n = 2$$

Similarly:

$$\int_0^{\infty} y^2 e^{-By^2} dy = \frac{1}{4B} \sqrt{\pi/B}$$

REFERENCES

1. Wolfendale, A. Brit. Proc. IEE, 1957.
2. Salzberg and Sard. Proc. IRE (letter), Oct. 1957.
3. McIntyre, R. J. J. of Appl. Phys., June 1961.
4. Henebry, M. Journ. of Sc. Instruments, 1960.
5. Haitz, et al. J. of Appl. Phys., June 1963.
6. Rose, D. J. Phys. Rev. 105, 1957
7. Ruge and Keil. J. of Appl. Phys., Nov. 1963.
8. Champlin, K. J. of Appl. Phys., July 1959.
9. Chynoweth, A. G. J. of Appl. Phys., July 1960.
10. Smith, R. A. Semiconductors, Cambridge University Press, 1959.
11. Loeb, L. B. Kinetic Theory of Gases, Chap. 4. Dover: 1961.
12. Shockley, W. J. B. S. T. J., Vol. 30, 1951.
13. Mott and Massey. Theory of Atomic Coll., Oxford University Press, 1933.
14. Conwell, E. M. Proc. IRE 11, 1952.
15. Dingle, B. Phil. Mag., Vol. 46, 1955.
16. Brookes, A. Advances in Electronics and Electron Phys., Vol. 8, 1955.
17. Chynoweth, A. G. J. of Appl. Phys., July 1960.
18. Shockley, W. Solid-State Electronics, Vol. 2, No. 1, 1961.
19. Haitz, R. Research Report, Shockley Lab, Clevite Co., Aug. 1963.
20. Tokuyama, T. Solid-State Electronics, Vol. 5, 1962.
21. McIntyre, R. J. loc. cit., page 986.
22. Prince, M. B. Phys. Rev., Vol. 81, 1951.
23. D. H. Menzel. Fundamental Formulas of Physics. Dover: 1960.
24. Jonscher, A. K. Progress in Semicond. Ed., A. F. Gibson, Heywood and Co., 1962.
25. Valdes, L. Physical Theory of Transistors. McGraw-Hill, 1961.

JUN 20 1969

UNIVERSITY OF ILLINOIS-URBANA
510.84 IL6R no. C002 no.156-163(1963
Internet report /



3 0112 088398117